

University of Louisville

## ThinkIR: The University of Louisville's Institutional Repository

---

Electronic Theses and Dissertations

---

12-2021

### Translating particulate hexavalent chromium-induced chromosome instability, loss of homologous recombination repair and targeting of RAD51 from human lung fibroblasts to human bronchial epithelial cells.

Idoia Meaza Isusi  
*University of Louisville*

Follow this and additional works at: <https://ir.library.louisville.edu/etd>



Part of the [Toxicology Commons](#)

---

#### Recommended Citation

Meaza Isusi, Idoia, "Translating particulate hexavalent chromium-induced chromosome instability, loss of homologous recombination repair and targeting of RAD51 from human lung fibroblasts to human bronchial epithelial cells." (2021). *Electronic Theses and Dissertations*. Paper 4011.  
<https://doi.org/10.18297/etd/4011>

This Master's Thesis is brought to you for free and open access by ThinkIR: The University of Louisville's Institutional Repository. It has been accepted for inclusion in Electronic Theses and Dissertations by an authorized administrator of ThinkIR: The University of Louisville's Institutional Repository. This title appears here courtesy of the author, who has retained all other copyrights. For more information, please contact [thinkir@louisville.edu](mailto:thinkir@louisville.edu).

TRANSLATING PARTICULATE HEXAVALENT CHROMIUM-  
INDUCED CHROMOSOME INSTABILITY, LOSS OF  
HOMOLOGOUS RECOMBINATION REPAIR AND  
TARGETING OF RAD51 FROM HUMAN LUNG  
FIBROBLASTS TO HUMAN BRONCHIAL EPITHELIAL  
CELLS

By

Idoia Meaza Isusi  
B.S University of the Basque Country, 2016  
M.S University of the Basque Country, University of  
Southampton, University of Liege and  
University of Louisville, 2018

A Thesis  
Submitted to the Faculty of the  
School of Medicine of the University of Louisville in Partial  
Fulfillment of the Requirements For the Degree of  
Master of Science in Pharmacology and Toxicology

Department of Pharmacology and Toxicology  
University of Louisville  
Louisville, Kentucky

December 2021

Copyright 2021 by Idoia Meaza Isusi

All rights reserved



TRANSLATING PARTICULATE HEXAVALENT CHROMIUM-  
INDUCED CHROMOSOME INSTABILITY, LOSS OF  
HOMOLOGOUS RECOMBINATION REPAIR AND  
TARGETING OF RAD51 FROM HUMAN LUNG  
FIBROBLASTS TO HUMAN BRONCHIAL EPITHELIAL  
CELLS

By

Idoia Meaza Isusi  
B.S University of the Basque Country, 2016  
M.S University of the Basque Country, University of  
Southampton, University of Liege and  
University of Louisville, 2018

A Thesis Approved on

September 3rd, 2021

by the following Thesis Committee:

---

John Pierce Wise, Sr., Ph.D.

---

Sandra S. Wise, Ph.D.

---

Lu Cai, Ph.D.

---

David W. Hein, Ph.D.

---

Calvin J. Kouokam, Ph.D.

---

Ke Jian Liu, Ph.D

## ACKNOWLEDGEMENTS

I would like to express my most sincere gratitude to my mentor Dr. John Pierce Wise, for the numerous opportunities and experiences he has provided me during these last years. His advice has been priceless, and I could not emphasize enough how great of a mentor he is, in so many aspects. I also would like to thank my lab-mates and friends, Sandra Wise, Jennifer Toyoda, Aggie Williams, Haiyan Lu, Calvin Kouokam and John Wise Jr. for their endless support and contributions to this project.

I would also like to acknowledge the love and support of my family and friends, back at home and here in Kentucky. Many thanks for supporting my dreams and motivate me to continue pursuing them during challenging times.

## ABSTRACT

### TRANSLATING PARTICULATE HEXAVALENT CHROMIUM-INDUCED CHROMOSOME INSTABILITY, LOSS OF HOMOLOGOUS RECOMBINATION REPAIR AND TARGETING OF RAD51 FROM HUMAN LUNG FIBROBLASTS TO HUMAN BRONCHIAL EPITHELIAL CELLS

Idoia Meaza Isusi

September 3, 2021

Particulate hexavalent chromium [Cr(VI)] is a well-established human lung carcinogen. RAD51, a key protein in homologous recombination repair pathway, is inhibited after prolonged exposure to Cr(VI), leading to an increase in chromosome instability after prolonged exposures in human lung fibroblasts. chromosome instability is the proposed driver of Cr(VI) carcinogenesis. Since tumors from chromate workers develop from epithelial cells, we sought to translate these findings from human bronchial fibroblasts to human bronchial epithelial cells. We hypothesized Cr(VI) inhibits RAD51 after prolonged exposure leading to an increase in chromosome instability in human bronchial epithelial cells (BEP2D). We characterized the cytotoxicity and measured intracellular Cr ion levels, chromosome instability and RAD51 response. Altogether, the data show, in BEP2D cells, Cr(VI) induces DNA double strand breaks and targets RAD51 leading to an increase in chromosome instability, successfully translating the outcomes seen in human bronchial fibroblasts to human bronchial epithelial cells.

## TABLE OF CONTENTS

	PAGE
ACKNOWLEDGMENTS.....	iii
ABSTRACT.....	iv
LIST OF FIGURES.....	vi
INTRODUCTION	
Lung Cancer and Metals.....	1
Exposure to Cr(VI) and its Adverse Health Effects.....	2
Physico-Chemical Properties of Chromium.....	4
Mechanism of Carcinogenesis.....	5
METHODS AND MATERIALS	
Chemicals and Reagents.....	9
Cell Culture.....	10
Preparation of Zinc Chromate and Cell Culture Treatments.....	10
Clonogenic Survival Assay.....	11
Chromosome Aberration Assay and Scoring Criteria .....	11
Intracellular Chromium Ion Measurement: Atomic Absorption Spectrometry.....	14
Neutral Comet Assay .....	15
Sister Chromatid Exchange Assay.....	16
Immunofluorescence.....	17
Statistical Analysis.....	19
RESULTS	
Intracellular Cr Ion Levels Increase in a Time and Concentration-Dependent Manner in Bronchial Epithelial Cells.....	20

Particulate Cr(VI) Is Cytotoxic in a Concentration-Dependent Manner in Bronchial Epithelial Cells.....	23
Particulate Cr(VI) Induces DNA Double Strand Breaks in Bronchial Epithelial Cells.	25
Particulate Cr(VI) Induces Time and Concentration-Dependent Increase of Chromosome Instability in Bronchial Epithelial Cells.....	27
Particulate Cr(VI) Targets RAD51 Foci after Prolonged Exposures in Bronchial Epithelial Cells.....	32
Prolonged Exposure to Particulate Cr(VI) Increased Inappropriate Accumulation of RAD51 in the Cytoplasm in Bronchial Epithelial Cells.....	34
Sister Chromatid Exchange Increase after Cr(VI) Exposure in Bronchial Epithelial Cells .....	36
Chromosome Instability and Targeting of RAD51 after Particulate Cr(VI) Exposure Translates from Fibroblasts to Bronchial Epithelial Cells.....	38
DISCUSSION .....	46
CONCLUSIONS .....	53
REFERENCES .....	54
CURRICULUM VITA.....	61

## LIST OF FIGURES

FIGURE	PAGE
1. Proposed Mechanism of Cr(VI)-induced Carcinogenesis .....	5
2. Types of Structural Chromosome Damage.....	13
3. Sister Chromatid Exchanges.....	17
4. Region of Interest Analysis in MAXIP Images.....	19
5. Intracellular Cr Ion Levels Increase in a Time and Concentration-Dependent Manner in Bronchial Epithelial Cells.....	22
6. Particulate Cr(VI) Reduced Relative Survival in a Concentration-Dependent Manner in Bronchial Epithelial Cells.....	24
7. Particulate Cr(VI) Increases Tail Intensity in Bronchial Epithelial Cells.....	26
8. Particulate Cr(VI) Increase Total Chromosome Damage in a Time and Concentration-Dependent Manner in Bronchial Epithelial Cells.....	29
9. Particulate Cr(VI) Increase Percent of Metaphases with Damage in a Time and Concentration-Dependent Manner in Bronchial Epithelial Cells .....	30
10. Particulate Cr(VI) Reduces RAD51 Foci after Prolonged Exposures in Bronchial Epithelial Cells.....	33
11. Prolonged Exposure to Particulate Cr(VI) Increases Inappropriate Accumulation of RAD51 in the Cytoplasm in Bronchial Epithelial Cells.....	34
12. Sister Chromatid Exchanges Increase after Particulate Cr(VI) Exposure in Bronchial Epithelial Cells.....	37
13. Chromosome Damage after Particulate Cr(VI) Exposure Translates from Fibroblasts to Bronchial Epithelial Cells.....	41
14. Percent of Metaphases with Damage after Particulate Cr(VI) Exposure Translates from Fibroblasts to Bronchial Epithelial Cells.....	43
15.. RAD51 Foci Inhibition after Particulate Cr(VI) Exposure Translates from Fibroblasts to Bronchial Epithelial Cells.....	45

## INTRODUCTION

### **Lung Cancer and Metals**

Lung cancer is the number one cause of cancer death in the US, for both men and women (Siegel et al., 2020). For many years, lung cancer has caused more cancer deaths than the next three greatest causes of cancer death combined [breast, prostate and colorectal cancer (Siegel et al., 2020)]. Contrary to the misperception that lung cancer is just a disease of smoking, in the US, about 20% of people that develop lung cancer disease have never smoked, approximately 30,000 people a year, (American Cancer Society, 2020). Therefore, a key to help reduce lung cancer related deaths is to investigate other sources of lung cancer, other than smoking.

One potential overlooked culprit for the development of lung cancer is metal pollution. Metals are known to cause respiratory cancers. For example, nickel, cadmium, arsenic, beryllium and hexavalent chromium [Cr(VI)] (Grimsrud et al., 2003, Mezynska et al., 2018, Marshall et al., 2007, IARC 1993, ASTDR 2012) are in the list of the eight most dangerous lung carcinogens in occupational settings (Driscoll, 2004). Metals are not only occupational hazards, but also ubiquitous in the environment due to the widespread use in industry, and, therefore, have the potential to harm not only workers, but also the general public. Despite the prevalent exposure risks, we don't fully understand how these metals induce cancer.

In this study, we investigated the toxicological effects of the carcinogenic metal, hexavalent chromium. The first epidemiological study evaluating Cr(VI) workers in 1948, found 21.8% chromate workers deaths were linked to respiratory cancers, which was 16 times higher than the prevalence in the control population (Kaiser, 1948). Since then, many studies have reported the incidence of lung cancer, and to a lesser extend nasal and sinus cancers (ASTDR, 2000). Because of its significant toxicity and widespread exposure Cr(VI) is listed among the top 20 on the Agency for Toxic Substances and Disease Registry (ATSDR) Substance Priority List and is classified by the International Agency for Research of Cancer (IARC) as Group 1 “known cause of cancer in humans”. Despite all this literature evidence indicating Cr(VI) is a human lung carcinogen and a health hazard, the mechanism of carcinogenesis is unknown.

### **Exposure to Cr(VI) and its Adverse Health Effects**

Chromium is present in earth’s crust and in the environment predominately in the trivalent form. In contrast, the vast majority of hexavalent chromium found in the environment originates from anthropogenic releases. Cr(VI) is the most desirable valence state for industries, such as, metallurgical, refractory and chemical (ASTDR, 2008), due to its physical and chemical properties: hardness, anti-rust properties and bright colors. Indeed, the properties are so desirable that it has been used in industry for over 200 years now. To obtain Cr(VI), industries extract Cr(III) from natural sources and transform it into Cr(VI) through oxidizing chemical processes, to produce chromates (Barnhart et al., 1997). Between the production of Cr(VI) by industries, the usage of Cr(VI) and release of Cr(VI) as a byproduct from things like, burning fossil fuels, chrome plating, electroplating, cement work, cooling towers leather tanneries, dyes and pigments, Cr(VI) is a widespread environmental and occupational contaminant.

Several reports have estimated the amount of Cr(VI) being released into the environment. For example, according to EPA 1009.35 metric tons of Cr(VI) are estimated to be released into the atmosphere in the US every year (ASTDR, 2012). Other studies reported even higher amounts of atmospheric Cr(VI) release, suggesting about 58,000 to 112,000 metric tons of chromium are estimated to be released every year (Jonhson et al., 2006), amount of which a third is thought to be in the hexavalent form (Kieber 2002). These reported anthropogenic sources, account for 60-70% of emissions of atmospheric chromium (ATSDR, 2008). Despite the extensive evidence showing high environmental Cr(VI), the Permissible Exposure Level (PEL) for Cr(VI), of 5  $\mu\text{g}/\text{m}^3$  for a 8 h worktime average established by Occupational Safety and Health Administration (OSHA) (OSHA 2006), does not account for environmental exposure risks and has not been reviewed since 2006.

Cr(VI) exposure is not only a health concern in occupational settings, but also is a concern to the general public exposed to environmental levels because Cr(VI) exposure is cumulative. Pathological studies have shown accumulation of Cr(VI) is best correlated to malignant development in bronchial sites rather than the exposure levels (Kondo et al., 2003). Therefore, a high dose during a short period of time can be equivalent to a low-dose lifetime environmental exposure (EPA, 2005), thus suggesting that PEL should account for occupational and environmental exposures.

Regarding the route of exposure of Cr(VI), although ingestion and dermal exposure to Cr(VI) can occur, inhalation is the primary route of exposure for Cr(VI) and is associated to most Cr(VI)-induced health risks, the most lethal being lung cancer. However, other noncancerous toxicological effects described in humans after Cr(VI) inhalation are epistaxis, chronic rhinorrhea, nasal itching and soreness, nasal mucosal atrophy, perforations and ulceration of the nasal septum, bronchitis, pneumoconiosis, decreased pulmonary function, and pneumonia (ASTDR, 2012).

Additionally, Cr(VI) is also associated with reproductive, gastrointestinal and developmental effects (Speer and Wise, 2018). All these adverse effects of Cr(VI) exposure suggest the need to investigate the mechanism of action of this metal.

### **Physico-Chemical Properties of Chromium**

Valence and solubility of Cr(VI) are two important characteristics that directly affect Cr toxicokinetics. The valence ranges from (-2 to 6) with the hexavalent and trivalent forms being the most physiologically stable (Kotas and Stasicka, 2000). From those valences, the hexavalent form can cross the plasma membrane and is the form associated with adverse effects (Figure 1).

Regarding solubility, less water-soluble Cr(VI) compounds, such as lead chromate, are the most potent carcinogens (ASTDR 2012). This concept is supported by epidemiological (Langard and Vigander 1983), cell culture (Wise et al., 2002, Holmes et al., 2006) and animal (Levy et al., 1986, Takahashi et al., 2005, Toya et al., 1999) studies. These less-water soluble compounds are more potent carcinogens than highly soluble chromates, because they have a longer retention time in the lung. They settle in lung bifurcation sites where they induce tumors (Ishikawa et al., 1994, Ishikawa et al., 1994b) by slowly dissolving extracellularly, thus releasing Cr(VI) oxyanion over time and exerting prolonged exposures (Wise et al., 1993, Xie et al., 2004).

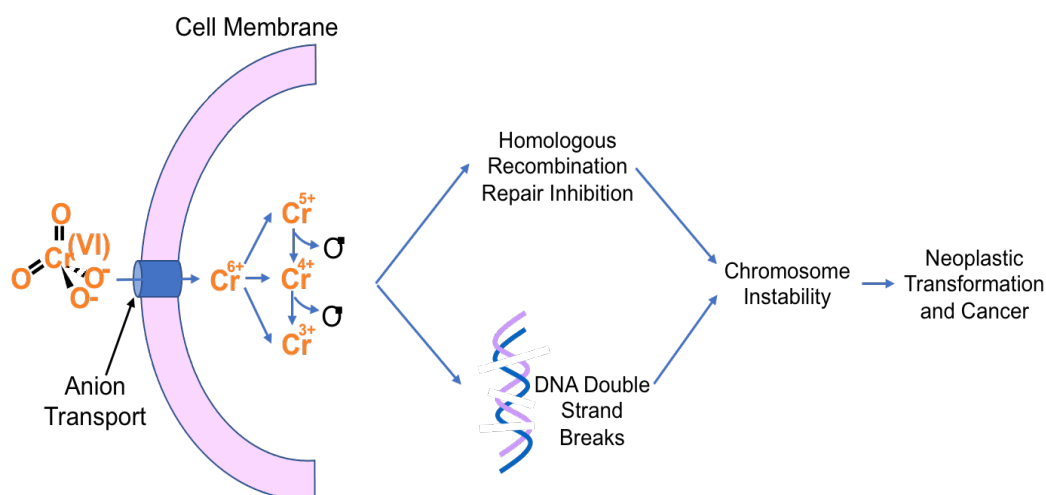


**Figure 1. Proposed Mechanism of Cr(VI)-induced Carcinogenesis**

This figure shows Cr(VI) enters the cell through anion transport by facilitated diffusion. Once inside the cells it gets rapidly reduced, generating Cr intermediates and reactive oxygen species. As a consequence, DNA double strand breaks are generated, and Cr exposure induces Homologous Recombination repair deficiency. Both outcomes lead to chromosome instability which is a predisposition to develop neoplastic transformation that can progress into cancer.

### Mechanism of Carcinogenesis

At the moment, the full mechanism of how Cr(VI) induces cancer is unknown. However, chromosome instability is considered the driving event in Cr(VI)-carcinogenesis. When Cr(VI) particles settle in bifurcation sites, they dissolve extracellularly and Cr(VI) oxyanion enters the cells through sulphate or phosphate anion channels by structural mimicry (Wise et al., 1993, Xie et al., 2004) (Figure 1). Once inside the cell, Cr(VI) is rapidly reduced into the next most stable state, Cr(III), through Fenton-like reactions. Fenton-like reactions consist of Cr(VI) reacting with H<sub>2</sub>O<sub>2</sub>, resulting in the reduction of chromium and production of hydroxyl radicals (HO·) (Chagas et al., 2019). The reduction process of Cr(VI) requires agents, such as, NADPH (Speer and Wise, 2018), ascorbate (Quevryn et al., 2003), glutathione (Wong et al., 2012) and thiol groups on cysteine (Zhitkovich et al, 2002). Reactive Oxygen Species (ROS) generated during the reduction of Cr(VI), lead to oxidative damage to major macromolecules, including nucleic acid, lipids and proteins (Speer

and Wise, 2018). Extracellular Cr(III) is bulky and poorly crosses the plasma membrane; similarly, intracellular Cr(III) is unable to exit the cell membrane (OSHA, 2006) and therefore, once inside the cell it can have deleterious effects. For example, *in vitro* studies show Cr(III) and Cr(V) have the ability to bind DNA (Stearns et al., 1995, Standeven and Wetterhahn, 1992), potentially creating Cr-DNA adducts, which if improperly repaired, can lead to stalled replication fork and DNA double strand breaks. The latter, is a common outcome reported by Cr(VI) literature (Qin et al., 2014, Wise et al., 2004a, Wise et al., 2002, Xie et al., 2009, Figure 1). DNA double strand breaks that are left unrepaired progress to chromosomal instability in Cr(VI) treated cells. Chromosome instability, a driver of Cr(VI) carcinogenesis and a hallmark of lung cancer, has been observed in tumors developed in chromate exposed workers (Hirose et al., 2002, Sarto et al., 1982, Xihoua et al., 2012).

Chromosome instability is a type of genomic instability. There are two forms of genomic instability: microsatellite instability and chromosome instability (Yao et al., 2014). There are two categories of chromosome instability: numerical and structural. Numerical chromosome instability refers to aberrant number of chromosomes, whereas structural chromosome instability refers to gross chromosome rearrangements, such as, additions, deletions and translocations, and are linked to replication stress, telomere dysfunction and errors in DNA break repair (Siri et al., 2021). Chromosome abnormalities might exist without being necessarily unstable. For example. Down syndrome patients have an addition of chromosome 21, however this is considered a stable aneuploidy and thus, is not considered chromosome instability.

An explanation for increased chromosome instability after Cr(VI) exposure is DNA repair deficiency. In a normal cell, DNA double strand breaks can be repaired by homologous recombination (HR) repair pathway, a high fidelity, template-

dependent pathway. Cr(VI)-induced DNA double strand breaks are preferentially repaired by HR (Tamblyn et al., 2009, Xie et al., 2008). Simplistically conceptualized, HR repair is constituted by a series of key steps: sensing step, transducing step and effecting step (D'Amours and Jackson, 2002). Briefly, during the sensing step, DNA double strand breaks are recognized by the MRN protein complex, which activates ATM by phosphorylation. ATM is involved in the transducing step, where it transmits the signal to downstream factors, such as, the histone variant H2A.X by phosphorylating it into  $\gamma$ H2A.X. This signal allows RPA to form a filament on the ssDNA, which is then substituted by RAD51 forming a filament. RAD51 is a recombinase protein and its filaments are key in the effecting step because it searches for the complementary strand by forming a D-loop to begin replication and repair of the broken site (D'Amours and Jackson, 2002). Thus, this repair pathway allows for DNA repair without any loss or addition of genetic material and prevents the progression of chromosome instability.

Data show Cr(VI) inhibits this pathway by targeting the effector protein RAD51 after prolonged (120 h) exposure in human lung fibroblast cells (Browning et al., 2016, Qin et al., 2014). The targeting of RAD51 by Cr(VI) after prolonged exposure results in unresolved breaks and increases in chromosome instability. The inability of the cell to repair breaks and the development of chromosome instability are key events in the mechanism of Cr(VI) carcinogenesis (Figure 1), as they are permanent and heritable phenotypes after Cr(VI) exposure (Wise et al., 2018).

These findings were described in WTHBF-6 cells, an h-TERT immortalized human bronchial fibroblast with diploid normal karyotype. This cell line is considered a robust model with stable karyotype and growth patterns. WTHBF-6 is the preferred model by literature to study the mechanism of Cr(VI) carcinogenesis (Wise et al., 2004b, Wise et al., 2018, Browning et al., 2016, Qin et al., 2014, Speer et al., 2021).

Importantly, this immortalized cell line responds to Cr(VI) in the same way as the parent primary human bronchial fibroblasts do, showing the same clastogenic and cytotoxic responses (Wise et al., 2004b).

Using fibroblast cells to investigate Cr(VI) carcinogenesis is relevant because Cr accumulates in fibroblast cells in tumors of chromate-exposed workers, and therefore are likely involved in the development of carcinogenesis (Kondo et al., 2003). However, since tumors in chromate workers originate from epithelial cells, we sought to investigate the effects of Cr(VI) in human bronchial epithelial cells. Previous findings in our lab show Cr(VI) transforms BEP2D cells, identified by loss of contact inhibition and gain of anchorage-independent growth (Xie et al., 2007). However, the effect of Cr(VI) exposure on the HR pathway in bronchial epithelial cells has not been tested yet. Therefore, the aim of this study was to translate chromosome instability and the targeting of RAD51 from human bronchial fibroblasts (WTHBF-6) cells to human bronchial epithelial cells (BEP2D). We hypothesized Cr(VI) inhibits RAD51 after prolonged exposure leading to an increase in chromosome instability in human bronchial epithelial cells.

## MATERIAL AND METHODS

### Chemicals and Reagents

LHC8 medium with or without gentamycin supplementation and gentamycin supplement were purchased from GIBCO. Buffer Tablets "GURR" were purchased from Gibco. TNS and 0.05% Trypsin/0.02% EDTA was purchased from Lifeline. Flasks and plasticware were purchased from Falcon. PBS was purchased from Corning. CometAssay® LMAgarose, CometSlide™ High Throughput Slides and CometAssay® Lysis Solution were purchased from R&D systems. Nitric Acid for Trace element analysis was purchased from Macron Fine Chemicals. Standard THGA Graphite tubes and Pure Chromium Standard were purchased from Perkin Elmer. Triton-X100, Proteinase K from Tritirachium album, Gelatin, 5-Bromo 2'-deoxyuridine were obtained from Sigma. Ethanol was purchased from Decon Labs. Methanol, Microcover glass, glass slides and sodium dodecyl sulfate (SDS) purchased from VWR. Acetic acid was purchased from J.T Baker. Potassium chloride, 4% paraformaldehyde in PBS was purchased from Alfa Aesar. Chamber Slide™ 4 chamber glass slide was purchased from Lab-Tek®II. ProLong™ Diamond Antifade Mountant with DAPI was purchased from Invitrogen. Giemsa was purchased from Ricca and J.T. Baker, respectively. Sodium azide purchased from Amresco. SYBR™ green was purchased from Lonza. Bovine serum albumin BSA was purchased from Calbiochem. Sodium chloride was purchased from EMD Millipore Corporation. Sodium citrate was purchased from Ward's Science. RAD51 rabbit polyclonal IgG was purchased from Santa Cruz Biotechnology and Alexa Flour 488 goat anti-rabbit IgG was purchased from Invitrogen.

Goat serum was purchased from MP Biologicals. Ammonium acetate and sodium acetate were purchased from VWR. EDTA tetrasodium was purchased from Acros Organics. Tris-Base from Sigma. Zinc chromate (CAS# 13530–65-9, 99.7% purity) was purchased from Pfaltz and Bauer (Lot Z00277, Waterbury, Connecticut).

### **Cell Culture**

Immortalized human bronchial epithelial cells, BEP2D were used in this study. BEP2D are E6/E7-immortalized human bronchial epithelial cells, a gift from Dr. Curtis Harris at the National Institute of Health (NIH). Cells were cultured as sub-confluent monolayers using LHC-8 medium in a 37°C humidified incubator with 5% CO<sub>2</sub>. All cell culture flasks and plasticware were coated with 0.1% gelatin for at least 1h before seeding the cells. Cells were fed every other day and subcultured every 3-4 days using 0.05% Trypsin/0.02%EDTA and Trypsin Neutralizing Solution (TNS). At the end of the experiments, cell confluency was between 70-90%. To ensure the authenticity of BEP2D cell line in our experiments, cells were karyotyped when thawed and after 3 months of continuous culturing. Additionally, cells were monitored for morphological changes, growth rate patterns, tested monthly for mycoplasma and short tandem repeat analysis was done yearly by American Type Culture Collection (Manassas, VA).

### **Preparation of Zinc Chromate and Cell Culture Treatments**

For all experiments in this study, zinc chromate was administered as a suspension in cold, sterile Millipore water as we previously described (Xie et al., 2009). Zinc chromate was weighed, added to 4°C sterile water and spun overnight at 4°C. The next day, dilutions were made from the stock vial while continuous vortexing, to avoid deposition of zinc chromate particles to the bottom of the vial and ensure homogeneous suspension. Cells were treated with concentrations ranging from 0 to 0.4 µg/cm<sup>2</sup> zinc chromate for 24 h and ranging from 0 to 0.2 µg/cm<sup>2</sup> zinc

chromate for 120 h. Cells were allowed to rest for 48 h after seeding, to resume logarithmic growth. Then medium was changed, and cells were treated. Treatments for prolonged (120 h) exposure, were administered each day for 5 days as follows: cells were rinsed with PBS to ensure removal of any treatment residue and new medium was added before treating with zinc chromate. Zinc chromate treatments were within environmentally relevant concentrations, but below occupational exposure limits as discussed before (Martino et al., 2015).

### **Clonogenic Survival Assay**

The clonogenic survival assay measures the ability of the cells to plate after Cr(VI) exposure. This assay is a gold standard in toxicology and the predominant assay used to determine Cr(VI) cytotoxicity in the literature (Meaza et al., 2020, Speer et al., 2018, Xie et al., 2015, Wise et al., 2010a,b). Briefly, cells were seeded into 6-well cell culture treated plates at appropriate seeding densities. Cells were allowed to rest for 48 h to resume logarithmic growth. Before treatment, medium was changed and cells were treated with 0, 0.1, 0.2, 0.3 and 0.4  $\mu\text{g}/\text{cm}^2$  for acute (24 h) exposure and 0, 0.05, 0.1, 0.15 and 0.2  $\mu\text{g}/\text{cm}^2$  for prolonged (120 h) exposure. At the end of treatment, cells were harvested, counted and reseeded. When reseeding cells, four 100 mm cell culture dishes per concentration were used at 500 cell densities. Dishes were fed every 5 days and once colonies were formed (7-10 days), dishes were fixed with methanol, stained with crystal violet, and colonies were counted. Three independent experiments were conducted.

### **Chromosome Aberration Assay and Scoring Criteria**

Clastogenicity was measured using the chromosome aberration assay according to our published methods (Wise et al., 2002,). Briefly, cells were seeded into 100 mm cell culture dishes and allowed to rest for 48 h to resume logarithmic growth. Before treatment with zinc chromate, medium was changed and cells were

treated with 0, 0.1, 0.2, 0.3 and 0.4  $\mu\text{g}/\text{cm}^2$  for acute (24 h) exposure and 0, 0.05, 0.1, 0.15 and 0.2  $\mu\text{g}/\text{cm}^2$  for prolonged (120 h) exposure. Demecolcine was added to the medium to arrest cell in metaphase one hour before end of treatment. Cells were then harvested and swollen with 0.075 M KCl hypotonic solution for 17 minutes and fixed with 3:1 methanol:acetic acid fixative for at least 30 minutes. Fixative was changed for new fixative 2 more times and cell suspension was then dropped onto clean, wet slides that were then placed on a humidifier (30% humidity, 30°C) to ensure consistent metaphase spreading. Slides were dried overnight and stained with 5% Giemsa diluted in Gurr's buffer pH 6.8. After allowing them to dry overnight, slides were coverslipped and metaphases were scored for chromosome aberrations using bright-field microscopy at x100 magnification. At least three independent experiments were conducted.

Chromosome aberrations were scored using previously described criteria (Wise et al., 2002). Chromosomal structural aberrations and numerical changes were counted in 100 metaphases in each treatment dose. Chromosomal instability consists of both structural and numerical chromosomal instability, and, therefore, in our analysis we measured both types of chromosome instability. Structural chromosome lesions consist of chromatid lesions (gaps and breaks), isochromatic lesions (gaps and breaks), dicentric chromosomes, rings, double minutes, acentric fragments, chromatid exchanges, fragmented chromosomes and centromere spreading (Figure 2). Results from structural lesions were expressed as total amount of chromosome damage in 100 metaphases scored and percent of metaphases with damage.

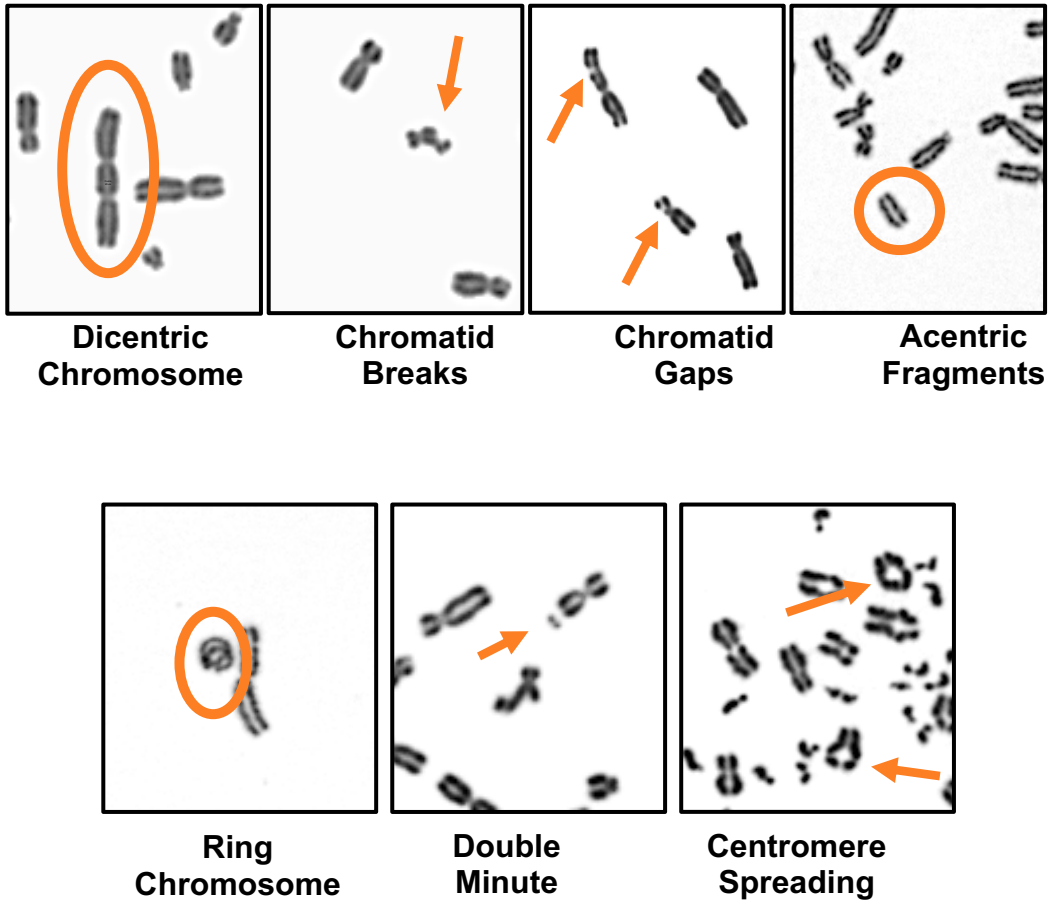


**Figure 2. Types of Structural Chromosome Damage**

This figure shows types of structural chromosome damage scored in the chromosome aberration assay. Some examples are: dicentric chromosomes, chromatid breaks and gaps, acentric fragments, ring chromosomes, double minutes and centromere spreading.

### **Intracellular Chromium Ion Measurement: Atomic Absorption Spectrometry**

Intracellular Cr ion levels were measured using atomic absorption spectrometry (AAS) following our previously published methods (Meaza et al., 2020). Briefly, cells were seeded into 60 mm cell culture treated dishes and allowed to resume logarithmic growth for 48 h. Medium was changed and cells were treated with 0, 0.1, 0.2, 0.3 and 0.4  $\mu\text{g}/\text{cm}^2$  for acute (24 h) exposure and 0, 0.05, 0.1, 0.15 and 0.2  $\mu\text{g}/\text{cm}^2$  for prolonged (120 h) exposure. A 0 h control was performed for all the zinc chromate treatments to account for particles passing through the 0.2  $\mu\text{m}$  filter and values were subtracted from the measurements obtained from 24 h and 120 h treatments. At the end of the treatment, 3 ml of cell culture supernatant was filtered through a 0.2  $\mu\text{m}$  filter for the determination of extracellular chromium ion levels. 2 ml of the filtered extracellular medium was then diluted with 2 ml of 2% trace element free nitric acid. Extracellular Cr ion concentration measurement allow us to determine whether treatments were performed correctly. For intracellular chromium ion levels, cells were harvested and counted with Multisizer Coulter counter. Cell number and diameter were recorded for the calculation of cell volume. Cell pellets were then washed twice with PBS, swollen with 0.075M KCl for 5 minutes and lysed with 2% SDS for 15 minutes. Then, cells were sheared with a syringe to ensure the complete breakdown of all cells and the release of intracellular medium. Lysate is then filtered with 0.2  $\mu\text{m}$  filter. 1.5 ml of intracellular medium is then diluted with 2.5 ml of 2% trace element free nitric acid.

Perkin Elmer 900Z graphite furnace atomic absorption spectrometer (GFAAS) with Syngistix Software was used. Standard curve calibration was performed in the AAS consisting of pure chromium at 0, 5, 10, 20, 40 and 80 ppb concentrations diluted in 2% trace element free nitric acid. The wavelength used for chromium was 357.87 nm, the limit of detection for chromium was 0.004  $\mu\text{g}/\text{l}$  and all data points were within the range of detection.

## Neutral Comet Assay

DNA double strand breaks were determined by single cell electrophoresis assay (neutral comet assay) adapted from our published methods (Meaza et al., 2020, Xie et al., 2005). Briefly, cells were seeded into 6-well cell culture treated plates and allowed to re-enter logarithmic growth for 48 h. Then, cells were treated with 0, 0.1, 0.2, 0.3 and 0.4  $\mu\text{g}/\text{cm}^2$  for acute (24 h) exposure and 0, 0.05, 0.1, 0.15 and 0.2  $\mu\text{g}/\text{cm}^2$  for prolonged (120 h) exposure. Thirty minutes before the end of the treatment, neocarzinostatin was added to one untreated well as a positive control for DNA double strand breaks. At the end of the treatment, cells were handled in the dark to avoid light induced damage. Cells were harvested, counted and resuspended in PBS in a 100,000 cells/ml concentration. The cell suspension was then mixed with warm low melting point LMAgarose® at 1:10 ratio. Cell-agar mixture was then mounted onto CometAssay® slides and chilled for 30 minutes at 4°C to allow solidification of the agar. Slides were submerged into CometAssay® lysis solution for 30 minutes at 4°C, rinsed with distilled water and incubated in proteinase K (1mg/ml) diluted in enzyme digestion solution for 2 h at 37°C. The enzyme digestion solution contained 2.5 M NaCl, 100 mM EDTA and 10 mM Tris adjusted to pH10. Slides were then rinsed and submerged into chilled electrophoresis buffer for 10 minutes. The electrophoresis buffer contained 0.1 M Tris Base, 0.3 M sodium acetate adjusted to pH 9. Electrophoresis was performed in CometAssay® units for 30 minutes, 21 V at 4°C. Slides were then rinsed with distilled water and immersed into DNA precipitation solution, containing 7.5 M 6.7 ml diluted into 43.3 ml of 200 proof ethanol for 30 minutes, followed by a 5 minutes step in 70% ethanol. Slides were dried overnight and were stained with 10,000X SYBR green diluted in TE buffer (10 mM Tris-base pH 7.5, 1 mM EDTA pH 7.5) for 30 minutes and rinsed with distilled water.

Cells were imaged using the Olympus Bx51 fluorescence microscope equipped with a SensiCam camera and taken with AVT Active Camera Viewer v1.0.8 (Allied Vision Technologies GmbH) as described before (Meaza et al., 2020). The configuration settings (brightness, shutter and gain) of the camera were consistent across different treatments within an experiment. Images were taken at 10x magnification and analyzed with CometAssay IV (Perceptive Instruments Lt). Tail intensity was measured in 100 cells per treatment and three wells were used (in 20 well CometAssay® slides) to analyze each treatment in order to ensure consistency. Experiments were repeated at least three times.

### **Sister Chromatid Exchange Assay**

HR repair activity was measured using a sister chromatid exchange (SCE) assay as we previously described (Browning et al., 2017). Briefly, cells were seeded in either 100 mm or 60 mm cell culture dishes and allowed to recover logarithmic growth for 48 h. Cells were treated with 0, 0.1, 0.2, 0.3 and 0.4  $\mu\text{g}/\text{cm}^2$  for acute (24 h) exposure and 0, 0.05, 0.1, 0.15 and 0.2  $\mu\text{g}/\text{cm}^2$  for prolonged (120 h) exposure. 5-Bromo 2'-deoxyuridine (BrdU) was added 48 h before the end of the treatment at 1 mg/ml concentration. Demecolcine was added to the medium to arrest cell in metaphase one hour before end of treatment. Cells were then harvested and swollen with 0.075 M KCl hypotonic solution for 17 minutes and fixed with 3:1 methanol:acetic acid fixative for at least 30 minutes. Fixative was changed with new fixative 2 more times and cell suspension was then dropped onto clean, wet slides that were then placed on a humidifier (30% humidity, 30°C) to ensure consistent metaphase spreading. Slides were then aged overnight and soaked in PBS for 5 minutes. Slides were then stained with 0.5  $\mu\text{g}/\text{ml}$  Hoechst 33258 pentahydrate solution for 10 minutes and incubated at 25  $\mu\text{g}/\text{ml}$  Hoechst 33258 pentahydrate solution under 27 W fluorescent light for at least 11 h. After incubation slides were then washed with distilled water and immersed in sodium chloride/sodium citrate

solution for 15 minutes at 60 °C. Slides were then rinsed with water and stained with 4% Giemsa in GURR's buffer for 5 minutes, dried overnight and coverslipped. SCEs were counted in 50 harlequin-stained metaphases per concentration (Browning et al., 2017) and experiments were repeated 3 times.

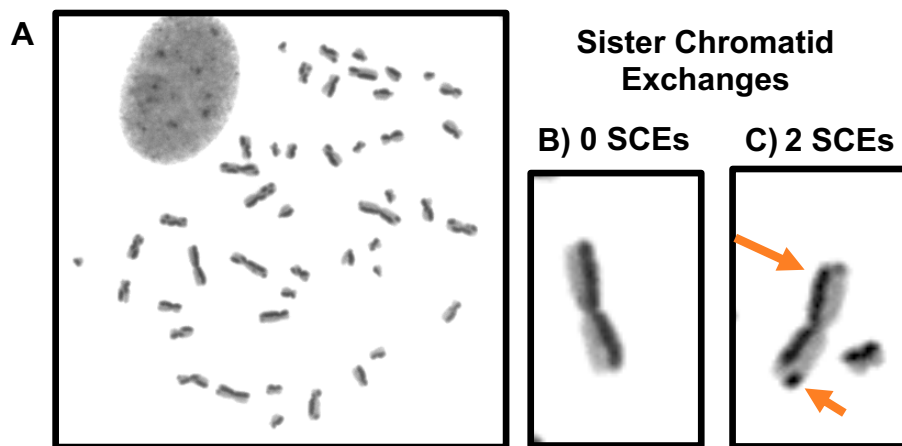


**Figure 3. Sister Chromatid Exchanges**

This figure shows how sister chromatid exchanges were scored in the harlequin-stained metaphases. **A)** Harlequin-stained metaphase **B)** Picture of a chromosome showing harlequin stain, with 0 sister chromatid exchanges **C)** Picture of a chromosome showing harlequin stain and two sister chromatid exchanges shown by arrows.

### Immunofluorescence

Immunofluorescent staining was performed according to our previously published methods, with some adaptations (Speer et al., 2021). Briefly, 4-well glass chamber slides were coated for at least 1 h with 0.1% gelatin. Cells were seeded and allowed to grow for 48 h to re-enter normal cell cycle pattern. Cells were treated with 0, 0.1, 0.2 and 0.4  $\mu\text{g}/\text{cm}^2$  for acute (24h) exposure and 0, 0.1 and 0.2  $\mu\text{g}/\text{cm}^2$  for prolonged (120 h) exposure. At the end of the treatment, medium was aspirated, and slides were rinsed with 1x PBS twice. Cells were fixed with 4% paraformaldehyde for 10 minutes and rinsed with PBS twice. Cells were permeabilized with 0.2% TritonX-100 for 5 minutes and rinsed with PBS twice. Slides were blocked with 10% goat serum in 1% BSA in PBS containing 10% sodium azide for 1h. Slides were washed

twice with PBS and primary antibody RAD51 was incubated overnight at 4°C at 1:200 concentration diluted in 1% BSA. After incubation, slides were washed 3 times for 5 minutes with PBS and secondary antibody Alexa Fluor 488 goat anti rabbit IgG was incubated for 1 h at 1:2000 in 1% BSA. Slides were washed 3 times for 5 minutes with PBS and dried overnight before mounting with Prolong Diamond Antifade Mountant with DAPI.

Two types of analyses were performed on RAD51 protein: 1) determination of foci and 2) cytoplasmic accumulation. RAD51 foci were counted by fluorescence microscopy in 100 cells per treatment. Results were expressed as number of cells with over 10 foci based on baseline levels. This threshold number ensures less than 5% of untreated controls had 10 foci or over. Cytoplasmic accumulation of RAD51 was measured using confocal microscopy and region of interest (ROI) analysis (Figure 4). Images of 50 cells per concentration were obtained using a Nikon A1 confocal laser microscope. The camera and laser conditions were kept constant within each experiment, and Z stacks were obtained with 60x objective and 0.75  $\mu\text{m}$  step size. A macro was created to process images as follows; first noise was reduced by Denoise-ai and second, z-stack images were compressed by creating maximum image projections (MAXIP). NIS-Elements was used to analyze the intensity of RAD51 in the cytoplasm and in the nucleus in processed images (Figure 4). Data was expressed as percent of cells containing higher value cytoplasmic accumulation than the control.

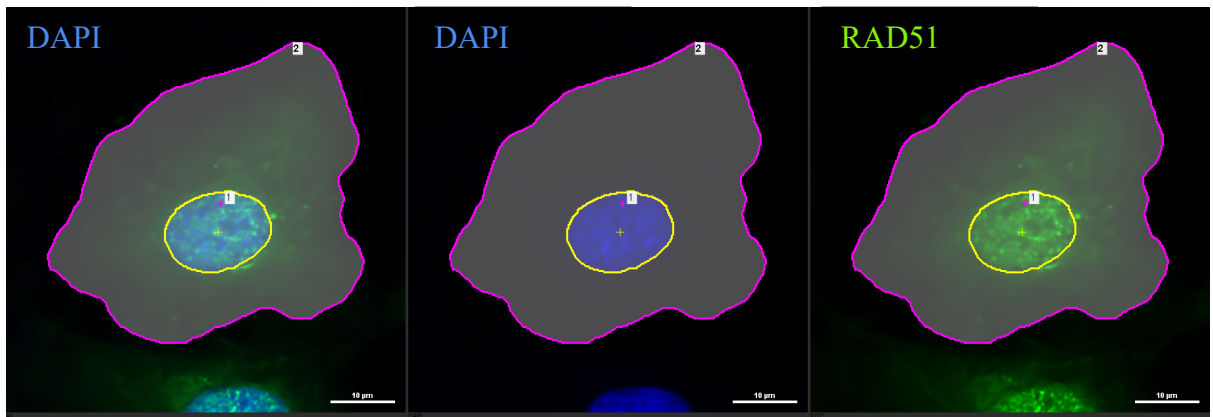


#### **Figure 4. Region of Interest Analysis in MAXIP Images**

This figure shows how region of interest analysis was performed in MAXIP images of RAD51 immunofluorescence in BEP2D cells. First, the nucleus was selected with automatic ROI setting using DAPI and was assigned ROI number 1. Then, the cytoplasm was traced free hand with an ROI tool and was assigned ROI number 2. ROI value from the nucleus was then subtracted from the ROI from the cytoplasm to yield the amount in the cytoplasm.

#### **Statistical Analysis**

Data were expressed as the mean  $\pm$  SEM (Standard Error of the Mean). Data were tested for homogeneity of variance with F-test. If data being compared were independent and had equal variances, Student-t test was performed. When variances could not be calculated or were not equal among the groups being compared, t-test assuming unequal variances was performed. For paired data, paired t-test was performed. Statistical significance was determined when  $p < 0.05$ .

## RESULTS

### **Intracellular Cr Ion Levels Increase in a Time and Concentration-Dependent Manner in Bronchial Epithelial Cells**

In order to translate Cr(VI) targeting of RAD51 and chromosome instability induction, intracellular Cr ion levels were measured to account for differential uptake of Cr(VI) between fibroblast and bronchial epithelial cells. Previous data show acute and prolonged exposure to Cr(VI) produces different intracellular Cr ion levels in human lung fibroblasts (Speer et al., 2019), leading to different toxic outcomes at each timepoint. Therefore, determining intracellular Cr levels was a critical step in the characterization Cr(VI) exposure to human bronchial epithelial cells.

We found intracellular Cr ion levels increase in a concentration-dependent manner (Figure 5A). Specifically, acute exposure to 0, 0.1, 0.2, 0.3 and 0.4  $\mu\text{g}/\text{cm}^2$  zinc chromate Cr(VI) resulted in 0, 63.5, 211, 427.5 and 839  $\mu\text{M}$  intracellular Cr levels, respectively. Prolonged exposure to 0, 0.05, 0.1, 0.15 and 0.2  $\mu\text{g}/\text{cm}^2$  zinc chromate, resulted in 1.3, 43, 161.5, 421.5 and 744  $\mu\text{M}$  intracellular Cr levels, respectively. Intracellular Cr ion levels also increased in a time-dependent manner. For example, exposure to 0.2  $\mu\text{g}/\text{cm}^2$  zinc chromate produced levels of 211 and 744  $\mu\text{M}$  after acute and prolonged exposure, respectively.

Zinc chromate is a particulate chromate compound and, therefore, is administered to the cells as a particulate suspension. Before administration to the cells, the zinc chromate stock solution is vortexed (as described in the methods section) to ensure homogeneity of the suspension. However, to ensure particle administration is consistent with treatment and similar between time points, we measured extracellular Cr ion levels. Notably, we found extracellular Cr levels were consistent with each treatment (Figure 5B).

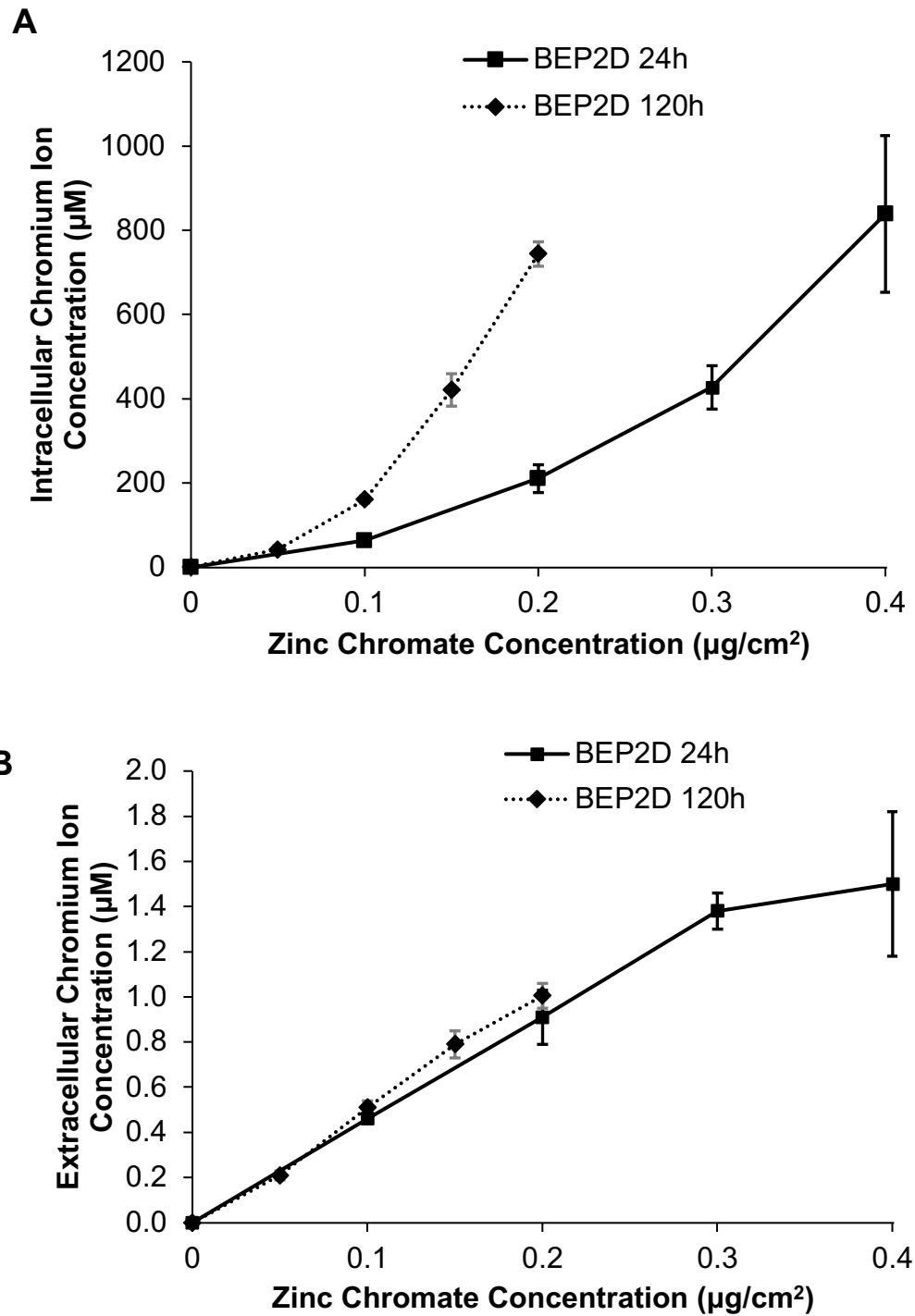


**Figure 5. Intracellular Cr Ion Levels Increase in a Time and Concentration-Dependent Manner in Bronchial Epithelial Cells**

This figure shows intracellular Cr ion levels in BEP2D cells after 24 h (solid line) and 120 h (dashed line) treatment with zinc chromate. Data are expressed as the mean of two independent experiments  $\pm$  standard error of the mean. \* =statistically different from control and plus sign (+) represents statistically different between time-points ( $p < 0.05$ ). **A**) intracellular Cr ion levels **B**) extracellular Cr ion levels.

## **Particulate Cr(VI) Is Cytotoxic in a Concentration-Dependent Manner in Bronchial Epithelial Cells**

Cytotoxicity was expressed as relative survival measured by clonogenic assay (Figure 6A). We observed a concentration-dependent decrease in cell survival. Specifically, after acute exposure to 0.1, 0.2, 0.3 and 0.4  $\mu\text{g}/\text{cm}^2$  zinc chromate, 85.3, 76.1, 64.4, and 15.3% survival was observed, respectively. Prolonged exposure to 0.05, 0.1, 0.15 and 0.2  $\mu\text{g}/\text{cm}^2$  zinc chromate resulted in 84.3%, 72.9%, 45.5% and 25.4% survival, respectively (Figure 6A). Statistical difference compared to control was observed in all except for the 0.1  $\mu\text{g}/\text{cm}^2$  after 24 h treatment. When comparing cell survival between time points only 0.2  $\mu\text{g}/\text{cm}^2$  was statistically different between acute and prolonged exposure. Differences in relative survival between acute and prolonged exposures to zinc chromate can be partially explained by differential uptake of Cr(VI) (Figure 6B).

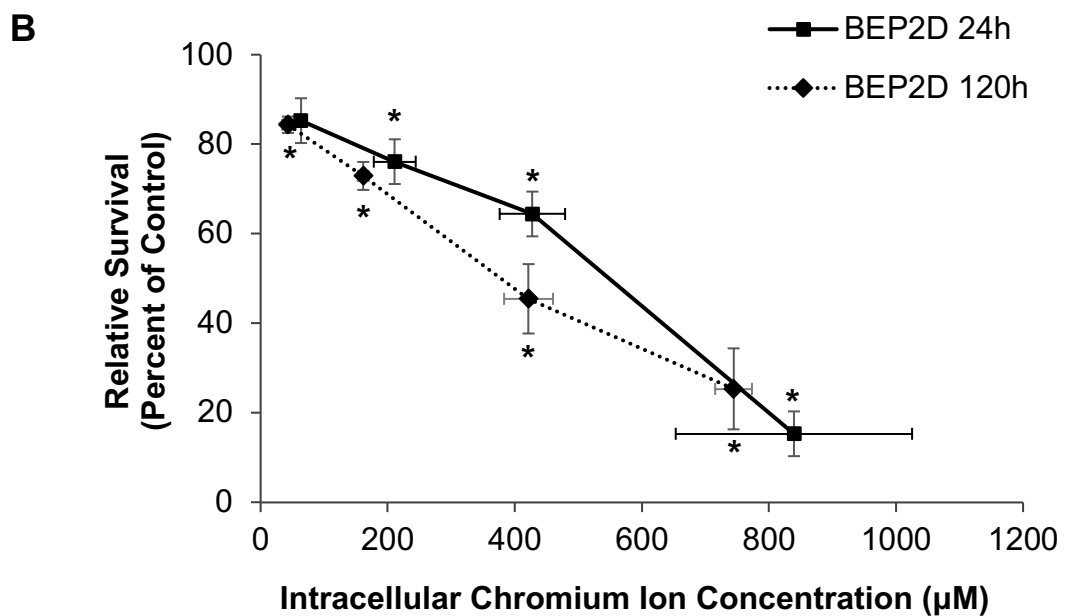
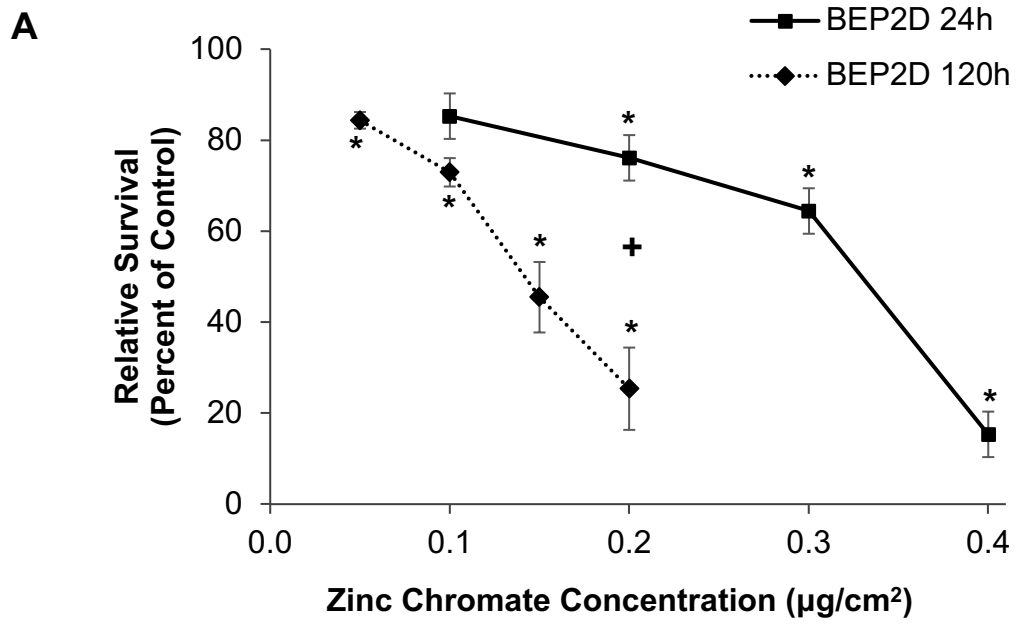


**Figure 6. Particulate Cr(VI) Reduces Relative Survival in a Concentration-Dependent Manner in Bronchial Epithelial Cells**

This figure shows the relative survival of BEP2D cells after 24 h (solid line) and 120 h (dashed line) treatment with zinc chromate. Data are expressed as the mean of three independent experiments  $\pm$  standard error of the mean. \* = statistically different from control ( $p < 0.05$ ), + = statistically different between time exposures ( $p < 0.05$ ). **A)** Relative survival based on administered dose. **B)** Relative survival based on intracellular Cr ion levels.

## **Particulate Cr(VI) Induces DNA Double Strand Breaks in Bronchial Epithelial Cells**

DNA double breaks are detrimental lesions that often occur after Cr(VI) exposure and when they are left unrepaired, can progress into chromosomal instability. In this study, DNA double strand breaks were measured with a neutral comet assay. DNA migrates through agarose via single cell electrophoresis and are quantified with SYBR green DNA stain. Data are then visualized as tail intensity. Data show particulate Cr(VI) induces DNA double strand breaks after acute and prolonged exposure to human bronchial epithelial cells (Figure 7). Specifically, acute exposure to 0.1, 0.2, 0.3, 0.4  $\mu\text{g}/\text{cm}^2$  zinc chromate induced 110, 110.3, 139.8, 151.7 % increase in tail intensity, respectively. Prolonged exposure to 0.05, 0.1, 0.15, 0.2  $\mu\text{g}/\text{cm}^2$  zinc chromate induced 122.1, 117.9, 135, and 161.7 % increase in tail intensity (Figure 7A). Differences in tail intensities between acute and prolonged exposures to zinc chromate (Figure 7A) can be explained by differential uptake of Cr(VI) (Figure 7B). Tail intensities after acute exposure to 0.3 and 0.4  $\mu\text{g}/\text{cm}^2$  zinc chromate were statistically different to controls, whereas no statistical difference was observed after prolonged exposure. Comparing tail intensities between acute and prolonged exposure, 0.2  $\mu\text{g}/\text{cm}^2$  zinc chromate treatment induced statistically bigger tail intensity after prolonged exposure. Neocarzinostatin (NCS) was used a positive control to ensure the procedure worked. The NCS in acute exposure experiments resulted in  $327.9 \pm 22.9$  increase in tail intensity whereas in the prolonged exposure experiments led to  $277.8 \pm 40.5$  increase.

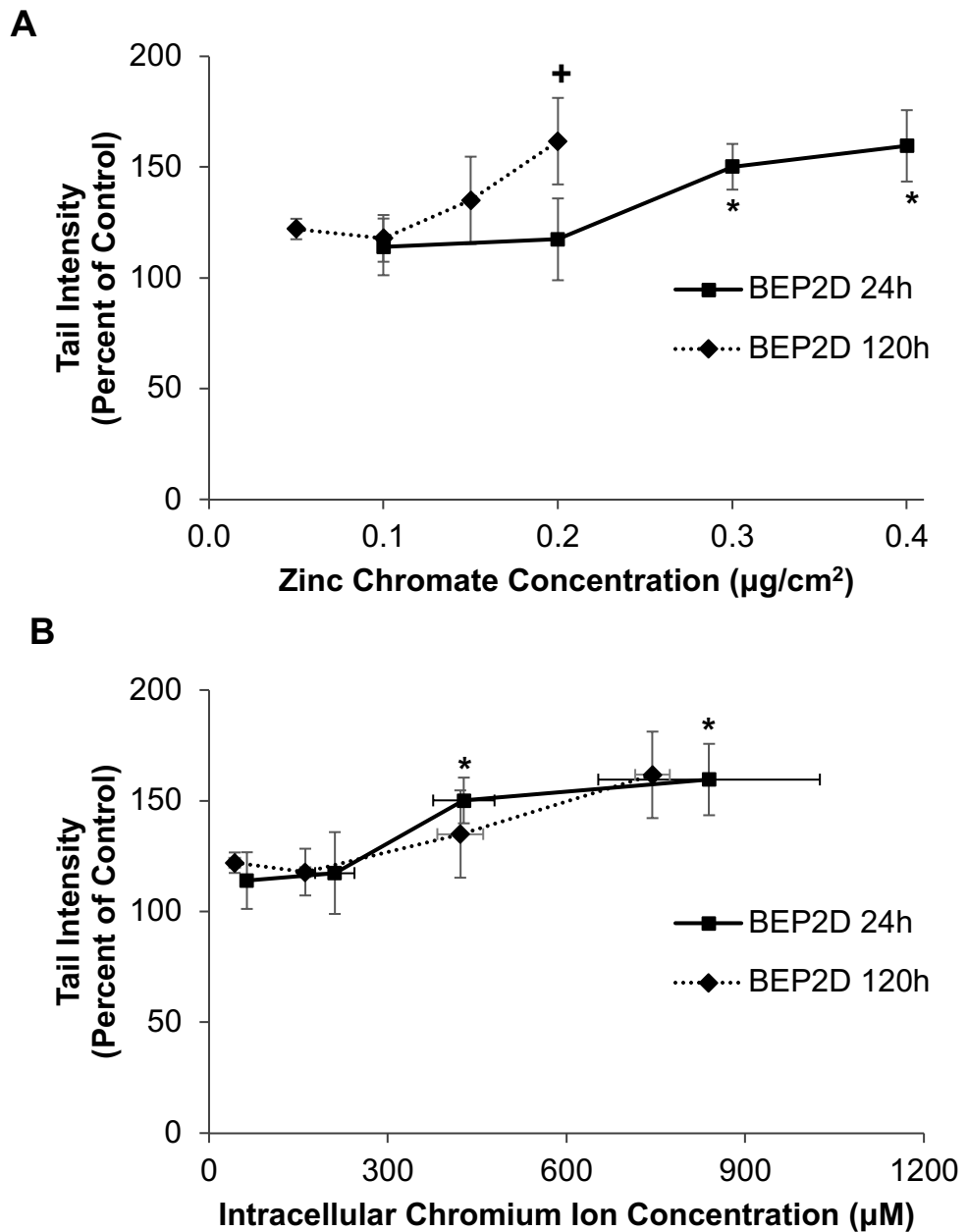


**Figure 7. Particulate Cr(VI) Increases Tail Intensity in Bronchial Epithelial Cells.**

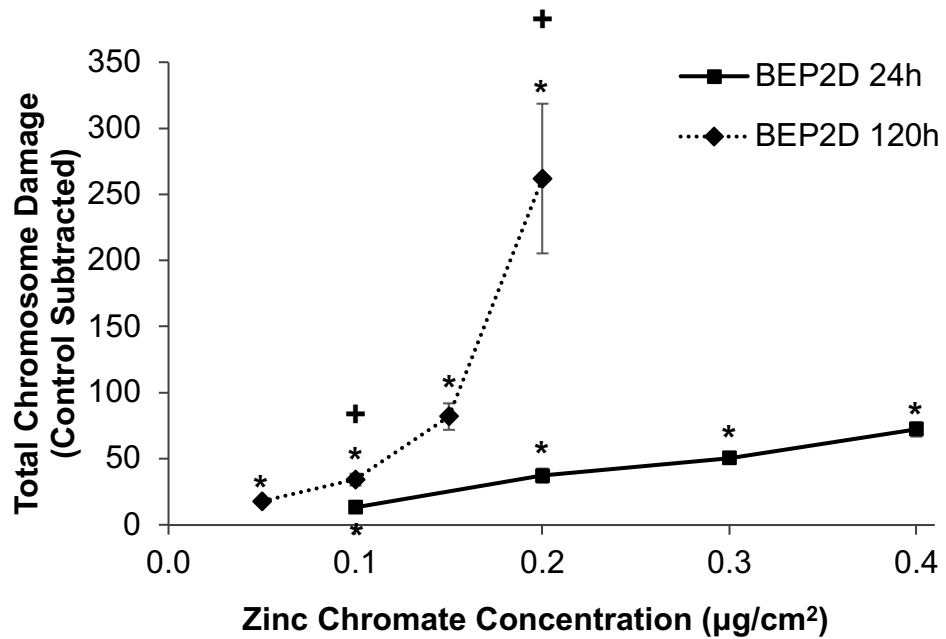
This figure shows the amount DNA double strand breaks measured with the comet assay in BEP2D cells after 24 h (solid line) and 120 h (dashed line) treatment with zinc chromate. Data are expressed as the mean of three (24 h) or two (120 h) independent experiments  $\pm$  standard error of the mean. \* = statistically different from control ( $p < 0.05$ ), + = statistically different between time exposures ( $p < 0.05$ ). **A**) Tail intensity as percent of control based on administered dose **B**) Tail intensity as percent of control based on intracellular Cr ion levels.

## **Particulate Cr(VI) Induces Time and Concentration-Dependent Increase of Chromosome Instability in Bronchial Epithelial Cells**

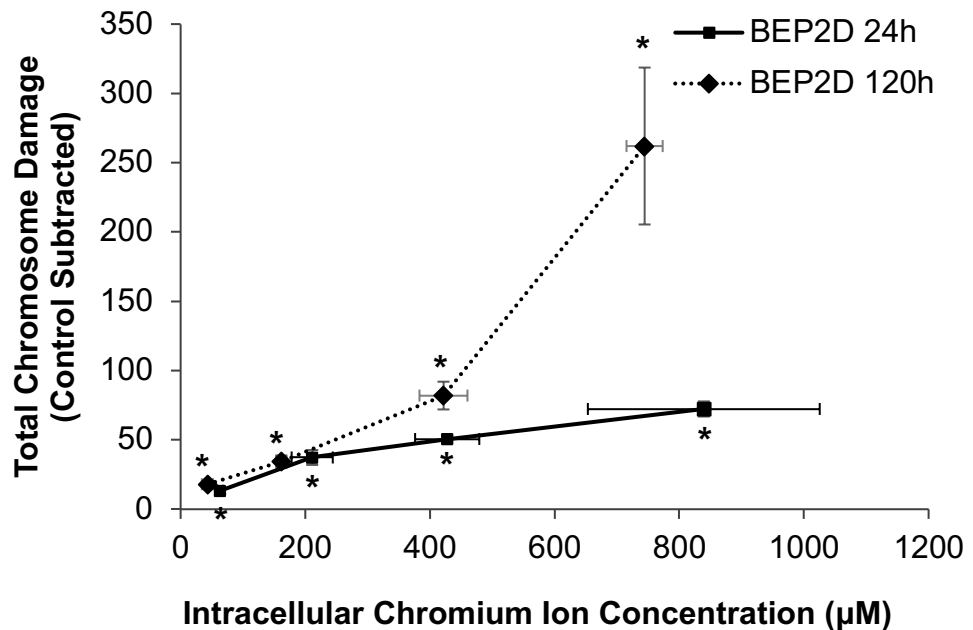
Chromosome instability is a key event proposed mechanism of Cr(VI) carcinogenesis (Proctor et al., 2014, Wise et al., 2018). We measured chromosome instability using a chromosome aberration assay, and observed particulate Cr(VI) exposure leads to a time and concentration-dependent increase of chromosome instability in bronchial epithelial cells (Figure 8 and 9). Data are represented in Figure 8 as the total amount of chromosome damage in 100 metaphases and in Figure 9 as the percent of metaphases with damage. Data show acute exposure to 0.1, 0.2, 0.3, 0.4  $\mu\text{g}/\text{cm}^2$  zinc chromate induced 13.3, 37.3, 50.7, and 72.3 chromosome aberrations, respectively (Figure 8A). On the other hand, prolonged exposure to 0.05, 0.1, 0.15, 0.2  $\mu\text{g}/\text{cm}^2$  zinc chromate induced 18, 34.3, 82 and 282 chromosome aberrations, respectively (Figure 8A). The most prevalent types of structural damage observed after 24 h exposure to zinc chromate were breaks, gaps, isochromatid breaks and gaps (Table 1). However, after prolonged exposure to zinc chromate, additional types of damage also emerged, such as dicentric chromosomes, double minutes and acentric fragments (Table 2). Statistical analysis showed, all the concentrations after both acute and prolonged exposure to Cr(VI) were statistically different from control. We also observed a time-dependent increase in chromosome damage. For example, 0.1  $\mu\text{g}/\text{cm}^2$  zinc chromate lead to 13.3 and 34.3 chromosome damage after acute and prolonged exposure respectively. Exposure time comparisons showed 0.1 and 0.2 were statistically different between acute and prolonged exposure. These differences in total chromosome damage between acute and prolonged exposures to zinc chromate (Figure 8A) cannot be explained by differential uptake of Cr(VI) (Figure 8B). These results suggest for the same amount of intracellular Cr, prolonged exposures develop more chromosome instability.

The percent of metaphases with damage showed similar trends compared to the amount of total chromosome damage. Acute exposure to 0.1, 0.2, 0.3 and 0.4  $\mu\text{g}/\text{cm}^2$  zinc chromate leads to 12.3, 28.3, 37.3 and 44.7% of metaphases containing damage, respectively (Figure 9A). Prolonged exposure to 0.05, 0.1, 0.15 and 0.2  $\mu\text{g}/\text{cm}^2$  zinc chromate induced 14.7, 28, 40 and 70.7% of metaphases containing damage, respectively (Figure 9A). Statistical analysis showed all concentrations at acute and prolonged exposures were statistically different compared to controls. Additionally, comparison timepoints, showed effects after 0.1 and 0.2  $\mu\text{g}/\text{cm}^2$  zinc chromate concentrations were statistically different between acute and prolonged exposure, where prolonged exposure resulted in more metaphases with damage. For example, exposure to 0.2  $\mu\text{g}/\text{cm}^2$  zinc chromate resulted in 28.3 and 70.7 metaphases with chromosome damage after acute and prolonged exposure, respectively. Similar to the results of total chromosome damage, differences in percent of metaphases with chromosome damage between acute and prolonged exposures to zinc chromate (Figure 9A) cannot be explained by differential uptake of Cr(VI) (Figure 9B). Total chromosome damage and percent of metaphases with chromosome damage data combined show at higher treatment concentrations not only is there more metaphases with damage, but metaphases contained more than one chromosome lesions.

**A**

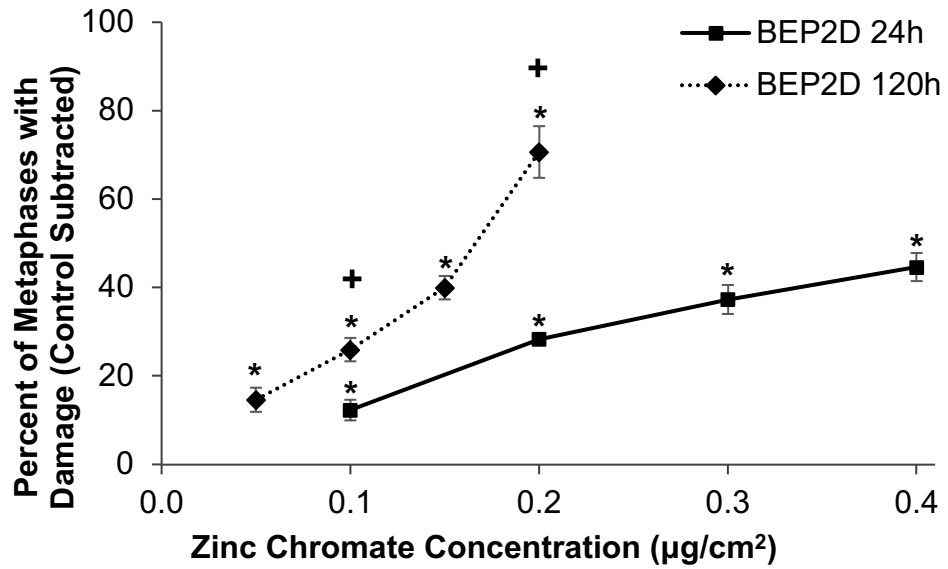
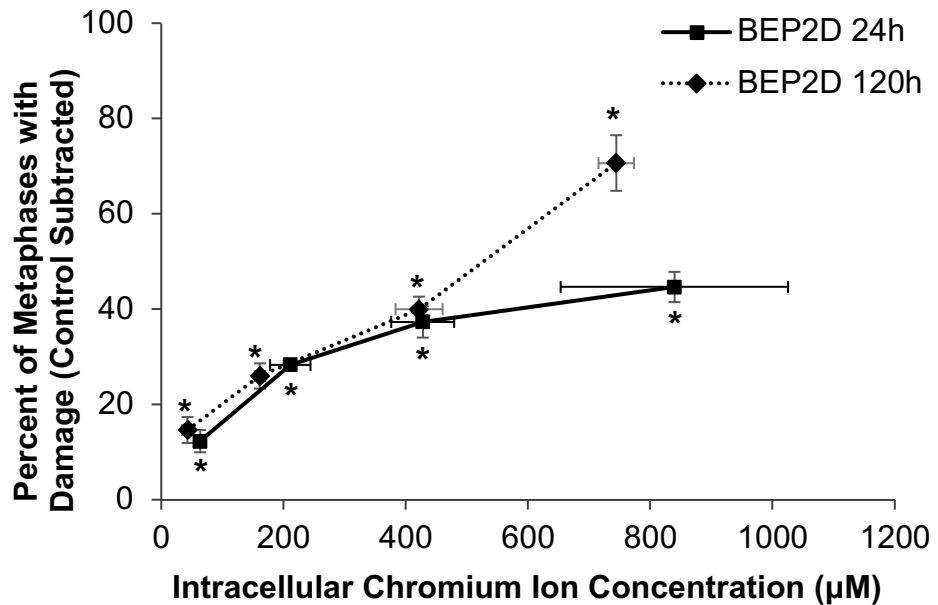


**B**



**Figure 8. Particulate Cr(VI) Increases Total Chromosome Damage in a Time and Concentration-Dependent Manner in Bronchial Epithelial Cells**

This Figure shows total chromosome damage in BEP2D cells after 24 h (solid line) and 120 h (dashed line) treatment with zinc chromate. Data are expressed as the mean of three independent experiments  $\pm$  standard error of the mean. \* = statistically different from control, + = statistically different between time exposures ( $p < 0.05$ ). **A)** Total chromosome damage based on administered dose. **B)** Total chromosome damage based on intracellular Cr ion levels.

**A****B**

**Figure 9. Particulate Cr(VI) Increases Percent of Metaphases with Damage in a Time and Concentration-Dependent Manner in Bronchial Epithelial Cells**

Shows percent of metaphases with chromosome damage in BEP2D cells after 24 h (solid line) and 120 h (dashed line) treatment with zinc chromate. Data are expressed as the mean of three independent experiments  $\pm$  standard error of the mean. \* = statistically different from control, + = statistically different between time exposures ( $p < 0.05$ ). **A**) Percent of metaphases with chromosome damage based on administered dose **B**) Percent of metaphases with chromosome damage based on intracellular Cr ion levels.

**Table 1.** Spectrum of chromosome aberrations induced after 24 h exposure to zinc chromate in human bronchial epithelial cells\* .

Zinc chromate concentration $\mu\text{g}/\text{cm}^2$	Chromatid Break	Chromatid Gap	Isochromatid Break	Isochromatid Gap	Chromatid Exchange	Ring	Dicentric	Double Minute	Acentric Fragment	Fragmented Chromosome	Centromere Spreading
0	3 $\pm$ 2.1	1.3 $\pm$ 0.7	0.3 $\pm$ 0.3	0	0	0	0	0	0	0	0
0.1	6.7 $\pm$ 3.3	8.3 $\pm$ 2.4	1.3 $\pm$ 0.7	1 $\pm$ 0.6	0	0	0.3 $\pm$ 0.3	0	0.3 $\pm$ 0.3	0	0
0.2	20.3 $\pm$ 7.4	15.7 $\pm$ 4.2	2.7 $\pm$ 1.2	1 $\pm$ 0.6	0.3 $\pm$ 0.3	0	0.7 $\pm$ 0.7	0	1.3 $\pm$ 0.3	0	0
0.3	30.3 $\pm$ 1.9	16.7 $\pm$ 1.2	2.7 $\pm$ 0.3	3 $\pm$ 1.2	0.7 $\pm$ 0.7	0	0.3 $\pm$ 0.3	0.7 $\pm$ 0.7	1 $\pm$ 0.6	0	0
0.4	37.7 $\pm$ 3.5	23 $\pm$ 0.6	7.7 $\pm$ 1.2	6.3 $\pm$ 3.8	1 $\pm$ 0.6	0	0.3 $\pm$ 0.3	0.7 $\pm$ 0.3	0.3 $\pm$ 0.3	0	0

\* Data represent mean of three independent experiments  $\pm$  standard error of the mean.

**Table 2.** Spectrum of chromosome aberrations induced after 120 h exposure to zinc chromate in human bronchial epithelial cells\* .

Zinc chromate concentration $\mu\text{g}/\text{cm}^2$	Chromatid Break	Chromatid Gap	Isochromatid Break	Isochromatid Gap	Chromatid Exchange	Ring	Dicentric	Double Minute	Acentric Fragment	Fragmented Chromosome	Centromere Spreading
0	0	1.3 $\pm$ 0.7	0	0.3 $\pm$ 0.3	0	0	0.3 $\pm$ 0.3	0	0	0	0
0.05	4 $\pm$ 2	9.3 $\pm$ 0.9	0.7 $\pm$ 0.3	0	0	0	4.7 $\pm$ 1.2	1.3 $\pm$ 0.9	0	0	0
0.1	11 $\pm$ 2.1	10.7 $\pm$ 1.8	1.7 $\pm$ 1.2	2.3 $\pm$ 0.3	0.3 $\pm$ 0.3	0	6.3 $\pm$ 0.9	1.3 $\pm$ 0.6	2 $\pm$ 1.5	0	0
0.15	29 $\pm$ 5.3	24.7 $\pm$ 0.3	5.3 $\pm$ 1.9	2 $\pm$ 0.6	0.0	0.0	6 $\pm$ 1.5	0.7 $\pm$ 0.3	2.3 $\pm$ 1.5	0.0	14.7 $\pm$ 14.7
0.2	176 $\pm$ 44	55.7 $\pm$ 9.5	12 $\pm$ 5.6	3.7 $\pm$ 0.7	1.7 $\pm$ 1.2	0.7 $\pm$ 0.3	4 $\pm$ 2	6.3 $\pm$ 4.5	4 $\pm$ 1.5	0.0	0

\* Data represent mean of three independent experiments  $\pm$  standard error of the mean.

## **Particulate Cr(VI) Targets RAD51 Foci after Prolonged Exposures in Bronchial Epithelial Cells**

We analyzed the ability of RAD51 to form foci because it is a key protein in the HR repair pathway. Previous studies showed prolonged exposure to Cr(VI) in human lung fibroblast cells inhibits RAD51 and reduces foci to baseline levels (Qin et al., 2014). Therefore, to translate this outcome to human bronchial epithelial cells, RAD51 foci were measured by immunofluorescence. First, we determined the baseline levels of RAD51 foci in untreated cells. We found, in bronchial epithelial cells, 95% of the untreated cells contained 10 foci or less. Therefore, for cells treated with particulate Cr(VI), we quantified the number of cells with more than 10 RAD51 foci, as previous work showed considering mean levels obscured effects. The data show acute exposure to 0, 0.1, 0.2 and 0.4  $\mu\text{g}/\text{cm}^2$  zinc chromate induced 5.7, 22, 29.3, 33.7 percent of cells with more than 10 RAD51 foci, respectively (Figure 10A). Prolonged exposure to 0, 0.05, 0.1 and 0.2  $\mu\text{g}/\text{cm}^2$  zinc chromate induced 1, 13.4, 14 and 18 percent of cells with more than 10 RAD51 foci (Figure 10A). Statistical analysis showed all concentrations after acute and prolonged exposure were statistically different to control. Remarkably, similar to the outcomes in fibroblast cells, prolonged exposure to particulate Cr(VI) resulted in inhibition of RAD51 compared with acute exposure after 0.2  $\mu\text{g}/\text{cm}^2$  zinc chromate. Specifically, 0.2  $\mu\text{g}/\text{cm}^2$  zinc chromate exposure led to 23.7 and 17 percent cells with over 10 RAD51 foci after acute and prolonged exposure, respectively. These differences in outcomes after acute and prolonged exposure were not due to differential uptake of Cr (Figure 10B).

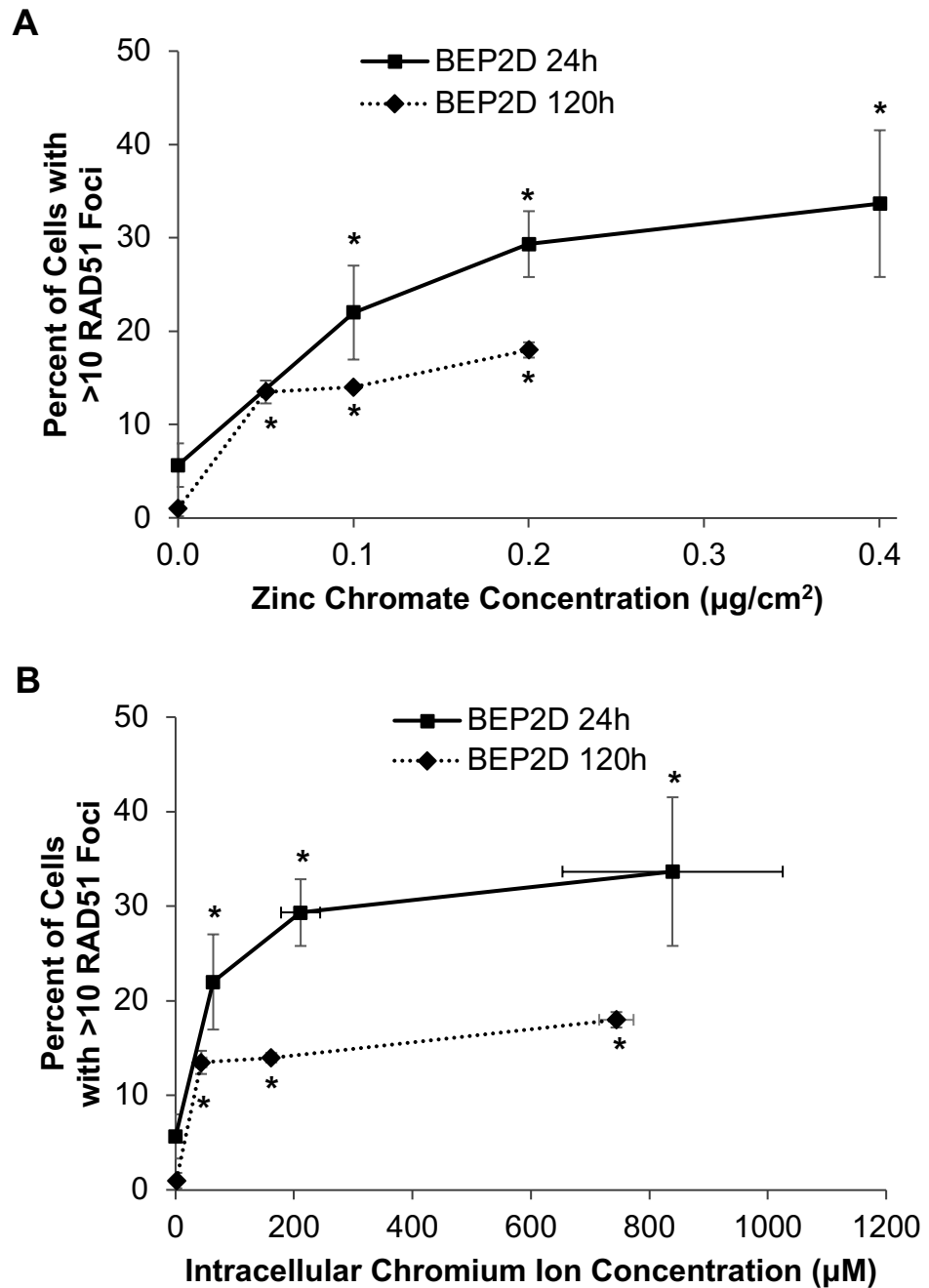


**Figure 10. Particulate Cr(VI) Reduces RAD51 Foci after Prolonged Exposures in Bronchial Epithelial Cells**

Shows percent of cells with >10 RAD51 foci in BEP2D cells after 24 h (solid line) and 120 h (dashed line) treatment with zinc chromate. Data are expressed as the mean of three (24 h) or two (120 h) independent experiments  $\pm$  standard error of the mean. \* =statistically different from control ( $p < 0.05$ ). **A**) Percent of cells with >10 RAD51 foci based on administered dose **B**) Percent of cells with >10 RAD51 foci in BEP2D cells based on intracellular Cr ion levels.

**Prolonged Exposure to Particulate Cr(VI) Increased Inappropriate  
Accumulation of RAD51 in the Cytoplasm in Bronchial Epithelial Cells**

Inhibition of RAD51 by prolonged Cr(VI) exposure is characterized by inability to form foci and inappropriate accumulation of RAD51 in the cytoplasm. Confocal imaging of Cr(VI) treated cells shows cytoplasmic accumulation increases after prolonged exposure to particulate Cr(VI). Specifically, acute exposure to 0.1, 0.2 and 0.4  $\mu\text{g}/\text{cm}^2$  zinc chromate induced cytoplasmic accumulation in 18, 13 and 15% of cells (Figure 11A). Prolonged exposure to 0.1 and 0.2  $\mu\text{g}/\text{cm}^2$  zinc chromate induced cytoplasmic accumulation in 10 and 44% of cells (Figure 11B). The difference between acute and prolonged exposure in cytoplasmic accumulation was not explained by correcting with intracellular Cr levels (Figure 11B).

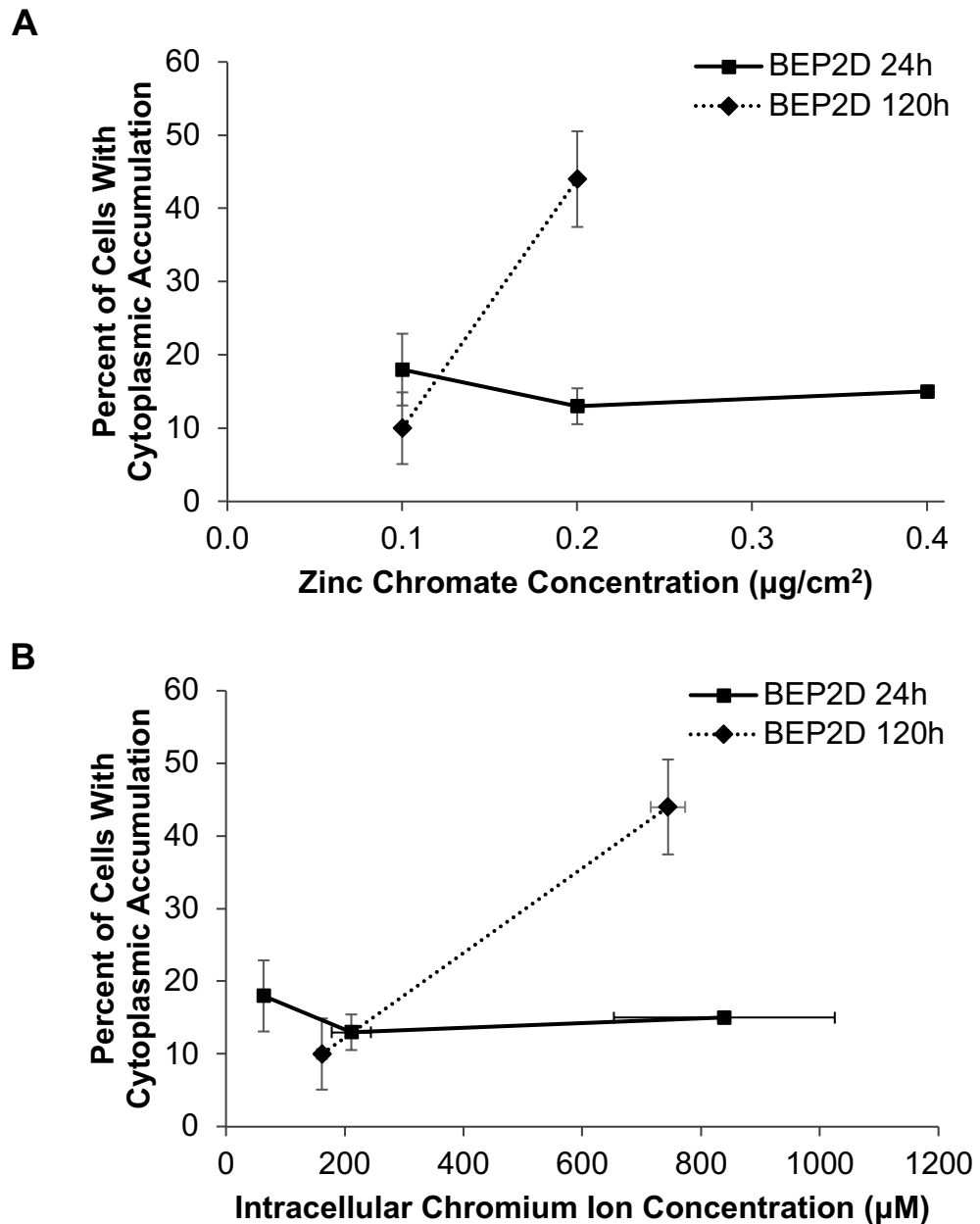


**Figure 11. Prolonged Exposure to Particulate Cr(VI) Increases Inappropriate Accumulation of RAD51 in the Cytoplasm in Bronchial Epithelial Cells**

This figure shows percent of cells with cytoplasmic accumulation of RAD51 in BEP2D cells after 24 h (solid line) and 120 h (dashed line). Data are expressed as the mean of two independent experiments  $\pm$  standard error of the mean. **A)** Percent of cells with cytoplasmic accumulation based on administered dose. **B)** Percent of cells with cytoplasmic accumulation based on intracellular Cr ion levels.

## **Sister Chromatid Exchange Increase after Cr(VI) Exposure in Bronchial Epithelial Cells**

Sister chromatid exchange (SCE) assay is a common assay used to measure HR repair. Contrary to the outcomes observed in lung fibroblasts where prolonged particulate Cr(VI) exposure reduces SCEs to background levels, data in epithelial cells show particulate Cr(VI) did not reduce SCEs after prolonged exposure. Specifically, acute exposure to 0, 0.1, 0.2, 0.3, 0.4  $\mu\text{g}/\text{cm}^2$  zinc chromate induced 10.4, 24.5, 36.2, 38.5 and 49.8 average SCE events per metaphase (Figure 12A). Prolonged exposure to 0, 0.05, 0.1, 0.15 and 0.2  $\mu\text{g}/\text{cm}^2$  zinc chromate induced 7.8, 33.1, 46.9, 51.1 and 57.4 average SCE events per metaphase (Figure 12A). All concentrations after acute and prolonged exposures were statistically different from controls. Prolonged exposure to 0.1  $\mu\text{g}/\text{cm}^2$  zinc chromate induced statistically relevant increase in SCEs than acute exposure. Intracellular Cr levels corrected some of the differences in SCE between acute and prolonged exposure to particulate Cr(VI) (Figure 12B).

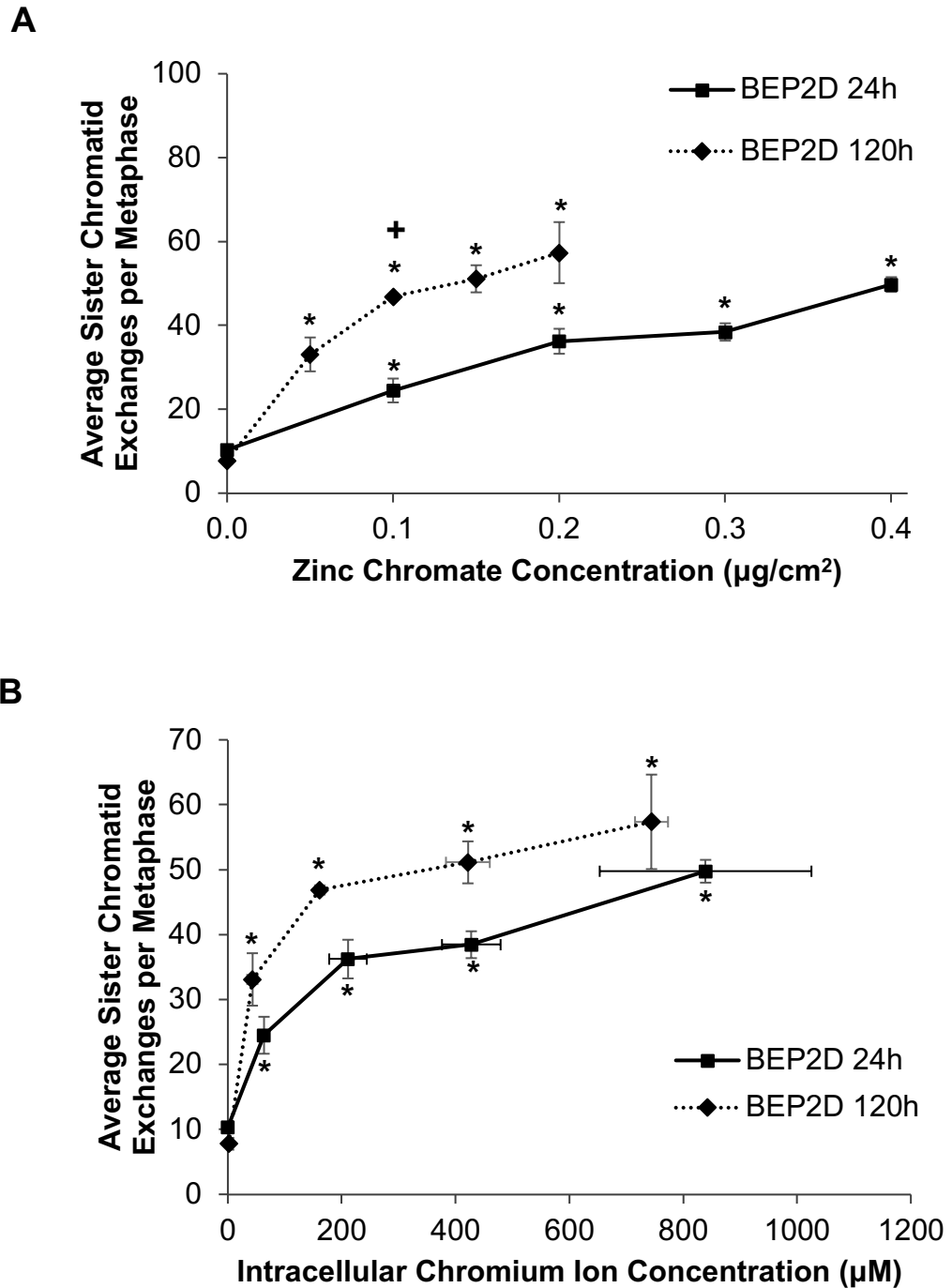


**Figure 12. Sister Chromatid Exchanges Increase after Particulate Cr(VI) Exposure in Bronchial Epithelial Cells**

This figure shows average sister chromatid exchange events per metaphase in BEP2D cells after 24 h (solid line) and 120 h (dashed line) treatment with zinc chromate. Data are expressed as the mean of three independent experiments  $\pm$  standard error of the mean. \* =statistically different from control ( $p < 0.05$ ), + = statistically different between time exposures ( $p < 0.05$ ). **A)** Average sister chromatid exchange events per metaphase based on administered dose. **B)** Average sister chromatid exchange events per metaphase based on intracellular Cr ion levels.

## **Chromosome Instability and Targeting of RAD51 after Particulate Cr(VI)**

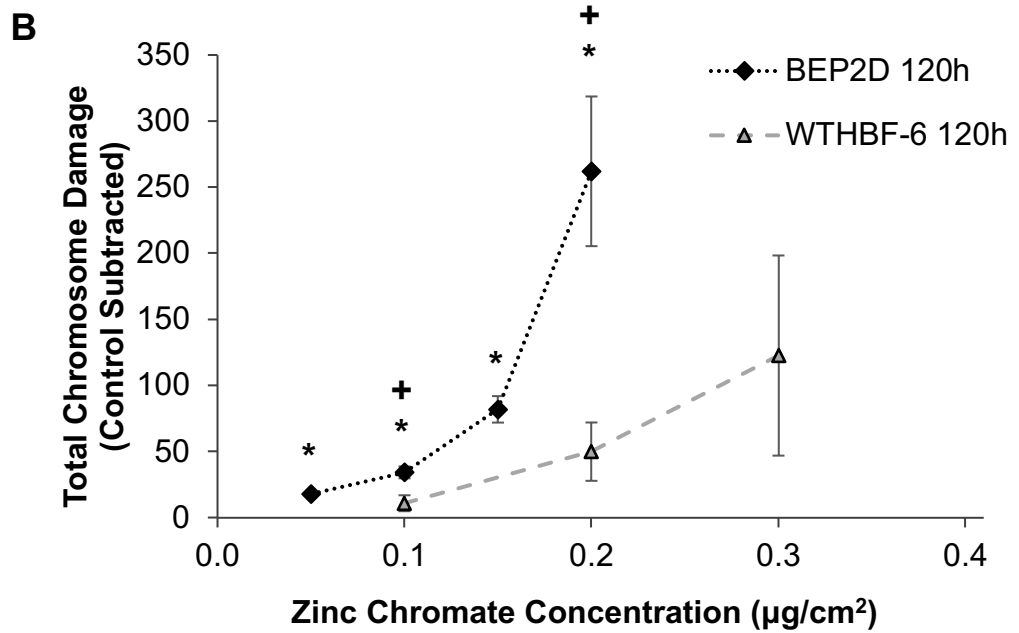
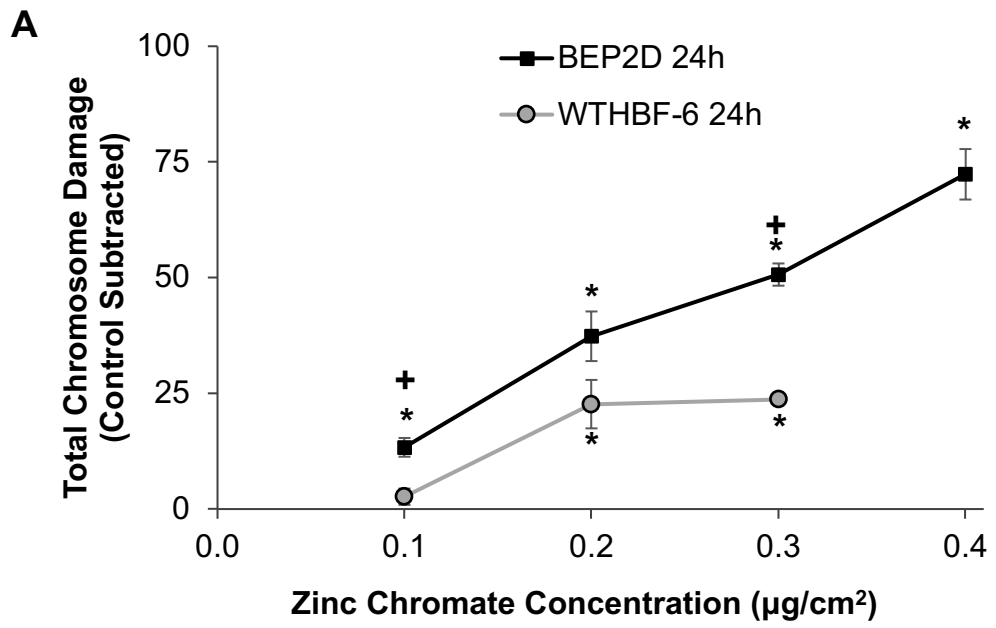
### **Exposure Translates from Fibroblasts to Bronchial Epithelial Cells**

The overall aim of this project is to translate outcomes from fibroblasts to bronchial epithelial cells. The data presented above show the outcomes do indeed translate. Here, we confirm the translation by directly comparing data from fibroblasts and epithelial cells based on two key events in the mechanism of Cr(VI) carcinogenesis: 1) loss of RAD51 function and 2) increased chromosomal instability (Wise et al., 2018, Browning et al., 2016). Figures 13, 14 and 15, directly compare results previously obtained in the lab in the human lung fibroblast cells (WTHBF-6 cells) with the current results of this project in human bronchial epithelial cells (BEP2D cells).

The data show the outcomes do translate from fibroblast cells to epithelial cells. In both cell types, we observe total chromosome damage and percent of metaphases with damage is larger after prolonged exposure to zinc chromate than acute exposure. For example, total chromosome damage after 0.2  $\mu\text{g}/\text{cm}^2$  zinc chromate exposure was 37.3 and 262 after acute and prolonged exposure in epithelial cells, respectively, while in fibroblast cells, exposure to the same concentration of zinc chromate resulted in 22.7 and 50 aberrations, respectively (Figure 13). Correction of differences by uptake of Cr showed the increase in chromosome instability after prolonged exposure cannot be explained by intracellular Cr levels for either cell line (Figure 13C,D and 14C,D). Additionally, effects on RAD51 function also translates from fibroblasts to epithelial cells (Figure 15). Acute exposure to zinc chromate results in a concentration-dependent increase in RAD51 foci in fibroblast and epithelial cells. For example, 0.1 and 0.2  $\mu\text{g}/\text{cm}^2$  zinc chromate cause 16.3 and 23.7 percent of cells with RAD51 in epithelial cells, respectively, and 22 and 29.7 percent of cells with RAD51 in fibroblasts, respectively (Figure 15). However, after prolonged exposure to Cr(VI) RAD51 foci formation is inhibited in

fibroblast and epithelial cells. For example, exposure to 0.2  $\mu\text{g}/\text{cm}^2$  zinc chromate induces 23.7 and 17 percent of cells with RAD51 after acute and prolonged exposure, respectively, in epithelial cells, and 29.7 and 3 in fibroblast, respectively (Figure 15).

Remarkably, the comparison of the two cell lines shows epithelial cells are more susceptible to chromosome instability after both acute and prolonged exposure to Cr(VI). For example, total chromosome damage after acute exposure to 0.2  $\mu\text{g}/\text{cm}^2$  zinc chromate resulted in 37.3 and 22.7 total chromosome damage in epithelial cells and fibroblast cells, respectively. This effect was more pronounced after prolonged exposure as 0.2  $\mu\text{g}/\text{cm}^2$  zinc chromate resulted in 262 and 50 total aberrations in epithelial cells and fibroblasts, respectively (Figure 13). This difference in susceptibility, has also been proven by percent of metaphases with chromosome damage (Figure 14) and was confirmed by statistical analysis. For example, we found acute exposure to 0.1 and 0.3  $\mu\text{g}/\text{cm}^2$  zinc chromate and prolonged exposure to 0.1 and 0.2  $\mu\text{g}/\text{cm}^2$  zinc chromate induced statistically significant increase in total chromosome damage in epithelial cells compared to fibroblast cells (Figure 13).



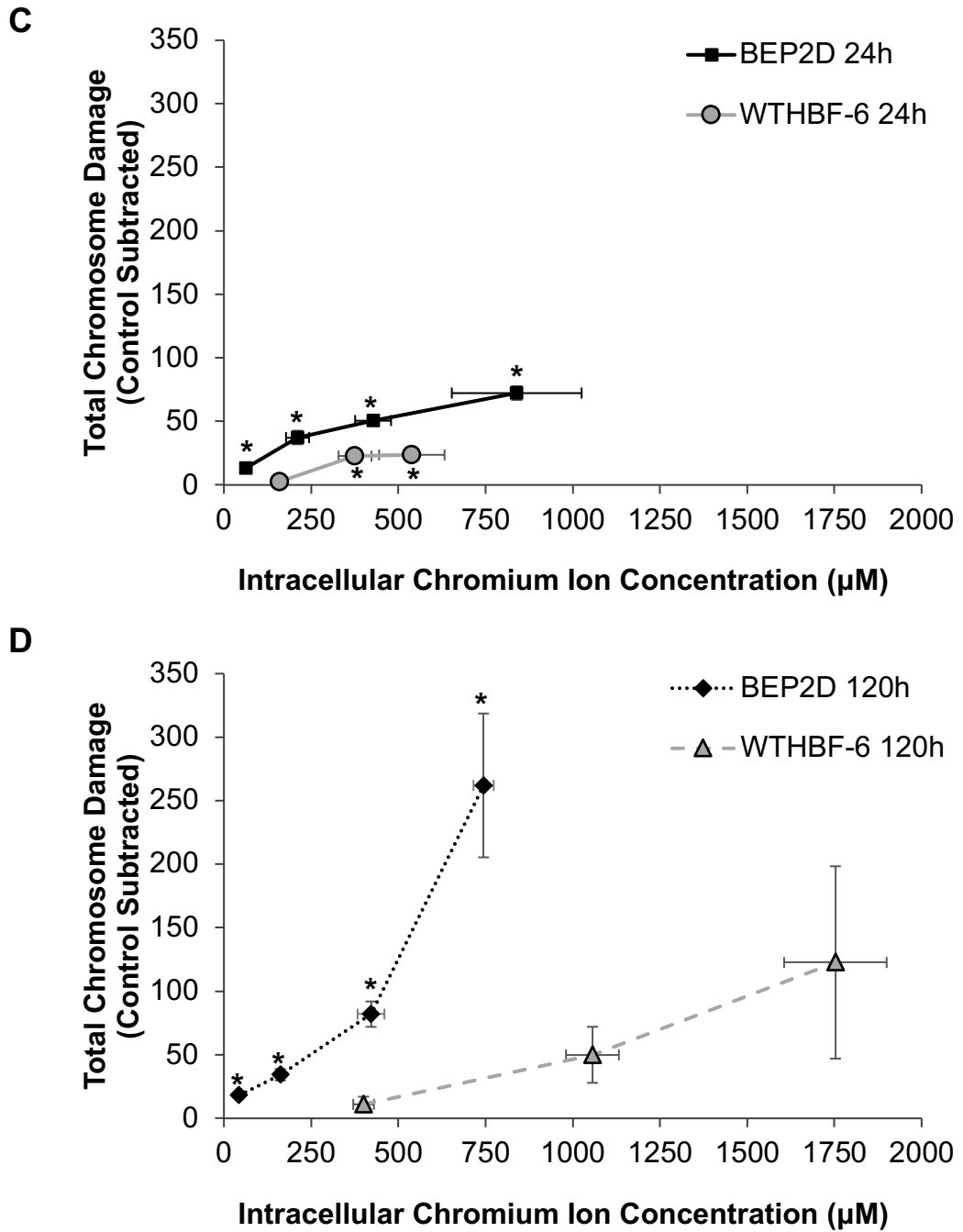
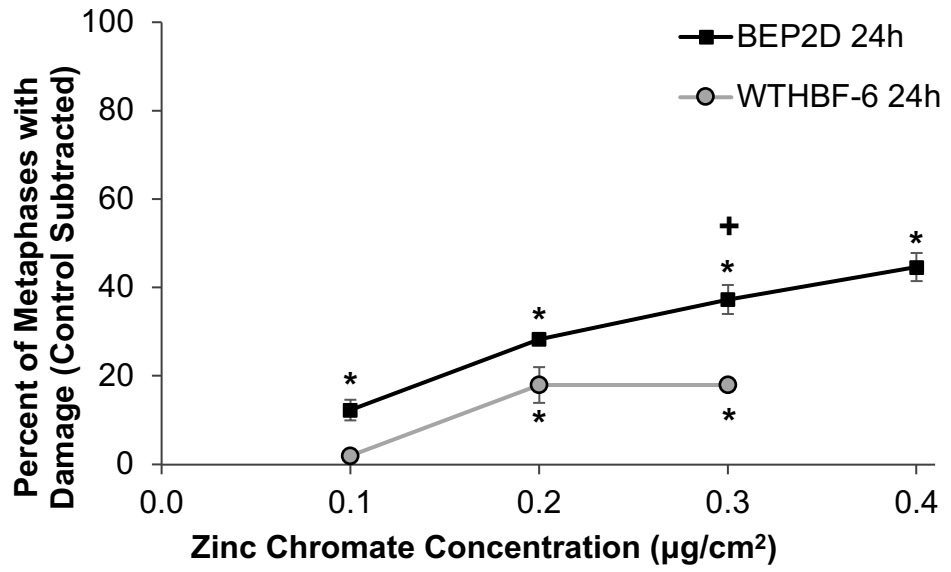


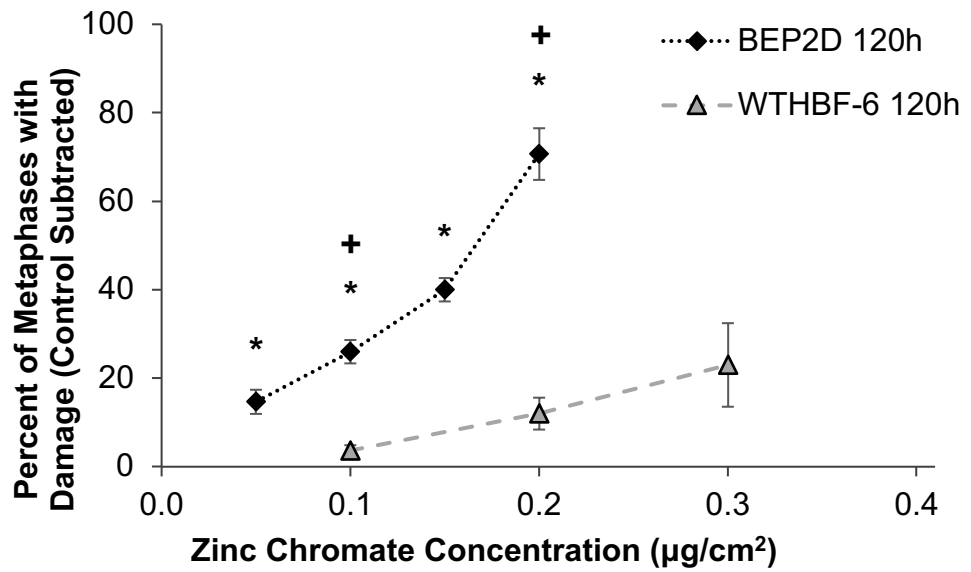
**Figure 13. Chromosome Damage after Particulate Cr(VI) Exposure Translates from Fibroblasts to Bronchial Epithelial Cells**

This figure shows total chromosome damage per 100 metaphases scored in BEP2D cells (black line) and WTHBF-6 cells (grey line) after 24 h (solid lines) and 120 h (dashed lines) treatment with zinc chromate. Data are expressed as the mean of three independent experiments  $\pm$  standard error of the mean. \* =statistically different from control ( $p < 0.05$ ), + = statistically different between time exposures ( $p < 0.05$ ). **A)** Total chromosome damage after 24 h treatment based on administered dose. **B)** Total chromosome damage after 120 h treatment based on administered dose. **C)** Total chromosome damage after 24 h treatment based on intracellular Cr ion levels. **D)** Total chromosome damage after 120 h treatment based on intracellular Cr ion levels.

**A**



**B**



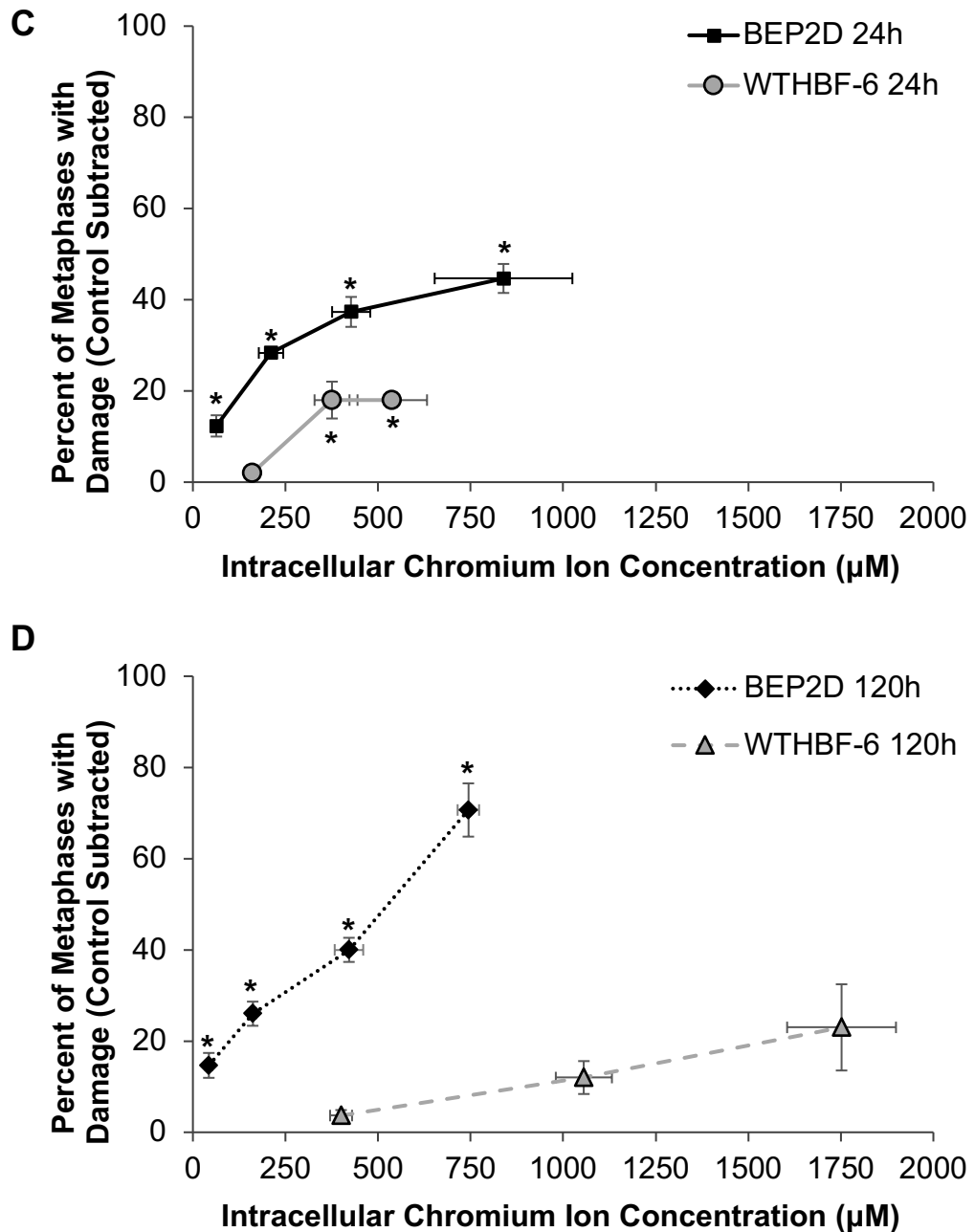
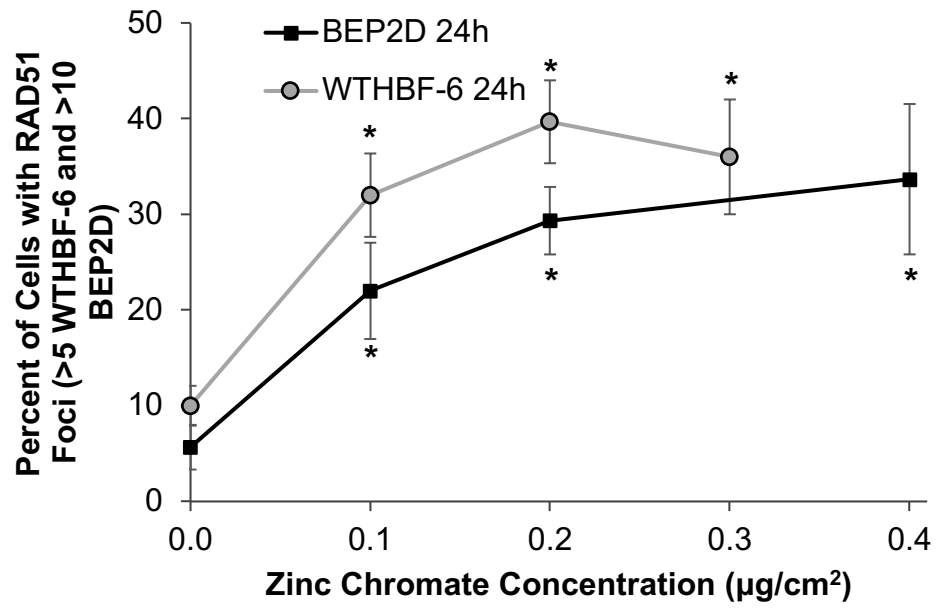
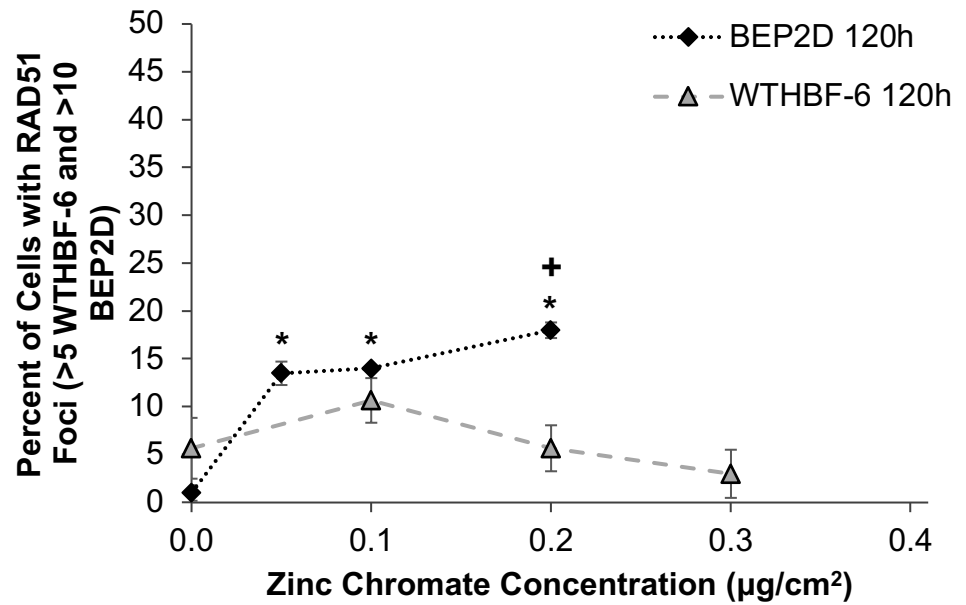


**Figure 14. Percent of Metaphases with Damage after Particulate Cr(VI) Exposure Translates from Fibroblasts to Bronchial Epithelial Cells**  
 This figure shows percent of metaphases with chromosome damage per 100 metaphases scored in BEP2D cells (black line) and WTHBF-6 cells (grey line) after 24 h (solid lines) and 120 h (dashed lines) treatment with zinc chromate. Data are expressed as the mean of three independent experiments  $\pm$  standard error of the mean. \* =statistically different from control ( $p < 0.05$ ), + = statistically different between time exposures ( $p < 0.05$ ). **A)** Percent of metaphases with chromosome damage after 24 h treatment based on administered dose. **B)** Percent of metaphases with chromosome damage after 120 h treatment based on administered dose. **C)** Percent of metaphases with chromosome damage after 24 h treatment based on intracellular Cr ion levels. **D)** Percent of metaphases with chromosome damage after 120 h treatment based on intracellular Cr ion levels.

**A**



**B**



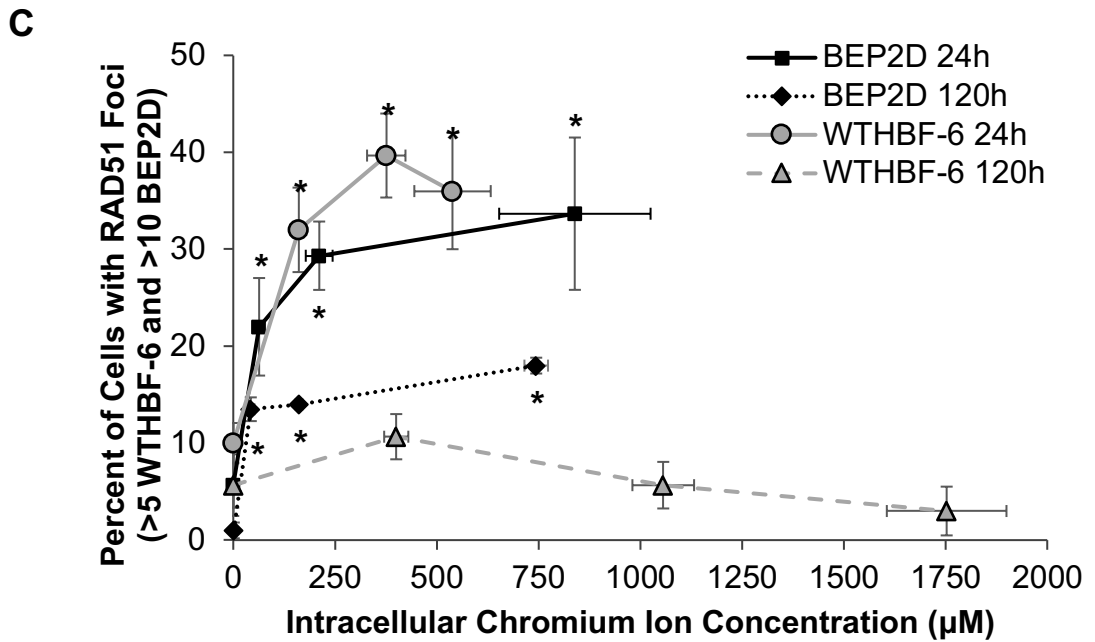


**Figure 15. RAD51 Foci Inhibition after Particulate Cr(VI) Exposure Translates from Fibroblasts to Bronchial Epithelial Cells**

This figure shows percent of cells with >5 RAD51 foci (WTHBF-6, grey) or >10 RAD51 foci (BEP2D, black) after 24 h (solid lines) and 120 h (dashed lines) treatment with zinc chromate. Data are expressed as the mean of three independent experiments  $\pm$  standard error of the mean. \* =statistically different from control ( $p < 0.05$ ), + = statistically different between time exposures ( $p < 0.05$ ). **A)** Percent of cells with RAD51 foci after 24 h treatment based on administered dose. **B)** Percent of cells with RAD51 foci after 120 h treatment based on administered dose **C)** Percent of cells with RAD51 foci after 24 h and 120 h treatment based on intracellular Cr ion levels.

## DISCUSSION

HR is a high-fidelity DNA repair pathway that helps prevent chromosomal instability, a defining event in the mechanism of Cr(VI)-induced carcinogenesis (Browning et al., 2016). Several studies have shown the importance of HR in protecting against metal exposure-induced chromosomal instability (Helleday et al., 2000, Zhang et al., 2014), and so is the case for Cr(VI) (Browning et al., 2016, Qin et al., 2014, Bryant et al., 2006, Stackpole et al., 2007). In HR repair pathway, RAD51 plays a crucial role on the nucleoprotein filament that aids on DNA strand invasion and complementary search steps (D'Amours and Jackson, 2002). Cr(VI) targets HR, by inhibiting RAD51, which is characterized by loss of RAD51 foci and increased cytoplasmic accumulation after prolonged exposure. Inefficient HR repair can lead to the use of alternative repair pathways such as the error prone NHEJ or SSA (Bennardo et al., 2008, Stark et al., 2004, Chang et al., 2017), leading to increased chromosomal instability (Browning et al., 2016). Although targeting of RAD51 and HR by Cr(VI) was demonstrated on human lung fibroblasts, there is no data on these effects in epithelial cells.

Bronchial epithelial cells play a central role in the mechanism of Cr(VI) carcinogenesis, because Cr(VI)-induced tumors originated from epithelial cells (Kondo et al., 2003). At the same time, biopsies of tumors derived from chromate exposed workers showed Cr actually accumulates in lung fibroblast cells, indicating these cells also play an important role (Kondo et al., 2003). This study is the first to consider particulate Cr(VI)-induced effects on RAD51 in human bronchial epithelial cells. Specifically, we observed particulate Cr(VI) targets RAD51 in epithelial cells decreasing RAD51 foci formation and increasing cytoplasmic accumulation after prolonged exposures.

In this study we demonstrated zinc chromate, our representative particulate Cr(VI) compound, is cytotoxic to human bronchial epithelial cells (BEP2D), which is consistent with previous studies. For example, potassium dichromate, a soluble chromate compound, is cytotoxic in a concentration-dependent manner to other human bronchial epithelial cells, such as, H460 cells (Krawic and Anatoly, 2018), small airway epithelial cells (Tessier et al., 2006) and BEAS-2B cells (Huang et al., 2017, Wu et al., 2011, Costa et al., 2010). Potassium chromate is also cytotoxic in a concentration dependent manner to H460 cells (Reynolds et al., 2012). Two studies looked at the effects of different solubilities of chromate compounds on cytotoxic outcomes (Borthiry et al., 2008, Wise et al., 2006). Borthiry et al., (2008) measured cytotoxicity after sodium chromate (soluble), zinc chromate (partially soluble) and lead chromate (water insoluble) in BEAS-2B and observed that all compounds induced concentration-dependent decrease in cell viability and the greater cytotoxicity was observed with increased solubility. This was further observed by Wise et al., (2006) in BEP2D cells after 24h exposure: soluble chromate (sodium chromate) induced more cytotoxicity than water insoluble chromate (lead chromate). However, no information on intracellular Cr ion levels were provided. Nevertheless, it is clear that Cr(VI) exposure is cytotoxic to bronchial epithelial cells.

Remarkably, only one study looked at cytotoxicity after prolonged exposure (120 h), where authors exposed BEP2D cells with lead chromate (Xie et al., 2007). Comparing to our results, to those from Xie et al., (2007), 10  $\mu\text{g}/\text{cm}^2$  exposure of lead chromate for 120h, leads to 46% relative survival, whereas our highest concentration 0.2  $\mu\text{g}/\text{cm}^2$  zinc chromate results in 25.4% relative survival. However, these outcomes and our study are difficult to compare for two main reasons: 1) the differences in solubility between lead chromate and zinc chromate will likely affect available Cr(VI) on the medium, therefore, intracellular Cr ion levels are needed to compare their outcomes to ours, 2) Xie et al., (2007) treated the cells with lead chromate only once at the beginning of the experiment, while in this study cell were treated daily for 120h. However, our data clearly shows that zinc chromate causes concentration-dependent and time-dependent decrease in cell viability and these results, also translate to fibroblast cells (Speer et al., 2019, Wise et al., 2010). Comparison between cytotoxic response after exposure to lead chromate, zinc chromate, sodium chromate or barium chromate showed that based on intracellular Cr ion levels, all compounds are cytotoxic in a concentration-dependent manner and zinc chromate is the most cytotoxic in human lung fibroblast cells (Wise et al., 2010).

Here, we demonstrated that Cr(VI) exposure induces genotoxicity in human bronchial epithelial cells. Four other studies have also reported similar outcomes before. For example, potassium chromate, induces micronuclei in H460 cells (Reynolds et al., 2012) and chronic exposure of potassium dichromate leads to aneuploidy in BEAS-2B cells (Rodrigues et al., 2009). Altogether, the data indicate 24 h exposure to Cr(VI) compounds in BEP2D cells induces concentration-dependent chromosome damage (Wise et al., 2006). Only one study investigated chromosome instability after prolonged exposure of Cr(VI) in BEP2D cells. This study showed, that 120 h exposure of lead chromate to BEP2D cells results in

chromosome instability and neoplastic transformation (Xie et al., 2007), indicating our study is consistent with previous literature showing the genotoxic potential of Cr(VI). Additionally, these results are also consistent with previous studies showing the same effect in human lung fibroblast cells (Wise et al., 2010)

The differences between acute and prolonged exposure in chromosome instability, were not explained by differential uptake of Cr between exposure times, suggesting the effect of Cr(VI) exposure is cumulative. These data correlate with previous findings showing effects of Cr(VI) exposure are best correlated to malignant development in bronchial sites rather than the exposure levels (Kondo et al., 2003). This study also revealed human bronchial epithelial cells are more susceptible to developing chromosome instability compared to fibroblast cells. This susceptibility could explain why tumors in chromate workers arise from epithelial cells (Kondo et al., 2003) and why these tumors are characterized by chromosome instability. A previous study showed Cr(VI) exposure to human bronchial epithelial cells transformed the cells and these cells were mostly (8 out of 9 foci) characterized with aneuploidy, a form of chromosome instability (Xie et al., 2007). Once more, this reiterates chromosome instability is a key step in the development of carcinogenesis.

Additionally, the time-dependent difference in response to Cr(VI) is also noticeable by a loss of RAD51 function after prolonged exposures. Acute exposure to particulate Cr(VI) induces an appropriate response to DNA damage, by increasing RAD51 foci and localizing it in the nucleus. In contrast, prolonged exposure to Cr(VI) induces a loss of RAD51 response, which is characterized by loss of RAD51 function and increased inappropriate cytoplasmic accumulation. These results agree with previous studies reporting the effect of Cr(VI) exposure in human lung fibroblast cells (Qin et al., 2014, Browning et al., 2016).

Loss of RAD51 foci after prolonged exposure can be explained by decreased availability of RAD51 in the nucleus, which is shown by our cytoplasmic accumulation data. However, why RAD51 accumulates on the cytoplasm after prolonged exposure to Cr(VI) is unclear. Previous data suggest Cr(VI) disrupts RAD51 mediators (Browning et al., 2016). RAD51 does not have a nuclear import amino acid sequence and therefore relies on proteins, such as, BRAC2 and RAD51C to be imported into the nucleus (Gildermeister et al., 2009, Jeyasekharan et al., 2013). Additionally, BRAC2 helps RAD51 load onto the single strand DNA and RAD51C stabilizes the RAD51 monofilament (Jensen et al., 2010, Amunugama et al., 2013). Previous data have shown Cr(VI) exposure does not affect BRAC2, but does inhibit RAD51C foci after prolonged exposure (Browning et al., 2016). Therefore, it is possible RAD51C inhibition prevents RAD51 from entering the nucleus leading to an inappropriate accumulation of RAD51 in the cytoplasm. Further work is needed to determine whether this is true.

In this study we investigated whether HR repair pathway is affected in epithelial cells after particulate Cr(VI) exposure by looking at RAD51 status and SCE events. We observed prolonged exposure to Cr(VI) targets RAD51 by inhibiting foci formation and inducing inappropriate accumulation in the cytoplasm in epithelial cells. However, the second measure of HR repair used in this study, SCEs, appeared to be not inhibited. There are several explanations to explain these outcomes. First, increased SCEs could be due to p53 inactivation in BEP2D cells. Although p53 status was shown not be related to SCE number in some studies (Wiktor-Brown et al., 2011, Bouffer et al., 1995, Bunz et al., 2002), others showed there is a link between p53 and SCEs (Cleaver et al., 1999, Sengupta et al., 2003, Prabhu et al., 2002). For example, it was shown SCE rate increased in cells transformed with E6 E7 proteins, which target p53 and Rb, and is the same immortalization procedure used in BEP2D cells (Cleaver et al., 1999). This effect, increase in SCEs due to p53

loss, was also observed in Bloom syndrome cells, which have loss of BLM and this effect was not seen in BLM positive cells, showing p53 and BLM interaction is linked to HR repair (Sengupta et al., 2003). It could be possible p53 alone might not induce increase in SCE, but the addition of other dysregulated genes, such as Rb or BLM can lead to aberrant SCEs.

Another explanation is that SCE assay might not be a good indicator of HR repair in epithelial cells. SCEs are widely used as a proxy for HR repair because they are considered a result of sister chromatid crossovers during HR repair (Sonoda et al., 1999). Sonoda et al., (1999) demonstrated HR is the principal cause of SCE events. However, there are different ways a DNA DSB can be solved by HR and not all the outcomes involve creation of SCE events (Li and Heyer 2008). For example, DNA DSB resolution by Double Holliday Junction(dHJ) recombination, a HR resolution where reciprocal DNA strand duplexes crossover and ligate to fix the breaks, can create SCEs events (Wilson and Thompson, 2000), but it is not the only resolution pathway in HR (Li and Heyer 2008, Agmon et al., 2011). Therefore, SCEs do not encompass all types of HR repair events.

Remarkably, involvement of p53 in inducing SCEs, can be explained by its role in Holliday Junction, Prabhu et al., (2002). p53 was shown to tightly bind to Holliday junctions (Lee et al., 1997), in low amounts, p53 binding to HJ, leads to a favorable conformation followed by cleavage of RuvC resolvase (Prabhu et al., 2002). However, at higher p53 concentrations, p53 prevents RuvC cleavage, probably due to the masking of the cleavage site by p53 or due to induction of non-productive conformation (Prabhu et al., 2002). This study suggests p53 tightly regulates HJs. Therefore, the loss of p53 in BEP2D cells could explain the increase in SCEs we are observing.

## CONCLUSIONS

In summary, these data suggest targeting of RAD51 and the increase chromosome instability after prolonged exposure to particulate Cr(VI) translates from human lung fibroblast cells to human bronchial epithelial cells. Chromosome instability is considered a key event in the development of Cr(VI)-induced cancer and in this study we show for the same amount of intracellular Cr levels, epithelial cells are more susceptible to the development of chromosome instability than fibroblast cells. This susceptibility could explain why tumors in chromate exposed workers originate from bronchial epithelial cells and are characterized with genomic instability. Additionally, in this study also we characterized the toxicological effects of particulate Cr(VI) exposure in human bronchial epithelial cells and will serve as a baseline for future mechanistic work on these cells. Studying human bronchial epithelial cells might provide better understanding on the role of epithelial cells on the mechanism of Cr(VI)-induced carcinogenesis.

## REFERENCES

Agency for Toxic Substances and Disease Registry (ATSDR). A Toxicological Profile for Chromium. U.S. Department of Health and Human Services, Public Health Service, Agency for Toxic Substances and Disease Registry; Atlanta, GA: 2012.

Agency for Toxic Substances and Disease Registry (ATSDR). Toxicological profile for Chromium. U.S. Department of Health and Human Services, Public Health Service, Agency for Toxic Substances and Disease Registry; Atlanta, GA: 2008.

Agency for Toxic Substances and Disease Registry (ATSDR). Case Studies in Environmental Medicine: Chromium Toxicity; U.S. Department of Health and Human Services: Atlanta, GA, 2000.

Agmon, N., Yovel, M., Harari, Y., Liefshitz, B., Kupiec, M. (2011). The role of Holliday junction resolvases in the repair of spontaneous and induced DNA damage. *Nucleic acids research*, 39(16), 7009–7019.

American Cancer Society (2020). Atlanta: American Cancer Society available in: <https://www.cancer.org/latest-news/why-lung-cancer-strikes-nonsmokers.html>

Amunugama R., Groden J., Fishel R. (2013). The HsRAD51B-HsRAD51C stabilizes the HsRAD51 nucleoprotein filament. *DNA Repair* 12, 723–732.

Barnhart, J. (1997). Occurrences, Uses, and Properties of Chromium. *Regulatory Toxicology and Pharmacology*, 26(1), S3-S7.

Bennardo N., Cheng A., Huang N., Stark J. M. (2008). Alternative-NHEJ is a mechanistically distinct pathway of mammalian chromosome break repair. *PLoS Genetics*. 4(6), e1000110.

Bouffler, S. D., Kemp, C. J., Balmain, A., Cox, R. (1995). Spontaneous and ionizing radiation-induced chromosomal abnormalities in p53-deficient mice. *Cancer research*, 55(17), 3883–3889.

Borthiry, G. R., Antholine, W. E., Myers, J. M., Myers, C. R. (2008). Reductive activation of hexavalent chromium by human lung epithelial cells: generation of Cr(V) and Cr(V)-thiol species. *Journal of inorganic biochemistry*, 102(7), 1449–1462.

Bryant, H. E., Ying, S., Helleday, T. (2006). Homologous recombination is involved in repair of chromium-induced DNA damage in mammalian cells. *Mutation research*, 599(1-2), 116–123.

Bunz, F., Fauth, C., Speicher, M. R., Dutriaux, A., Sedivy, J. M., Kinzler, K. W., Vogelstein, B., Lengauer, C. (2002). Targeted inactivation of p53 in human cells does not result in aneuploidy. *Cancer research*, 62(4), 1129–1133.

Browning, C. L., Qin, Q., Kelly, D. F., Prakash, R., Vanoli, F., Jasin, M., Wise, J. P., Sr (2016). Prolonged Particulate Hexavalent Chromium Exposure Suppresses Homologous Recombination Repair in Human Lung Cells. *Toxicological sciences: an official journal of the Society of Toxicology*, 153(1), 70–78.

Browning C.L., Wise C.F., Wise J.P. Sr. (2017) Prolonged particulate chromate exposure does not inhibit homologous recombination repair in North Atlantic right whale (*Eubalaena glacialis*) lung cells. *Toxicology and Applied Pharmacology* 331,18-23.

Chagas, P., Caetano, A. A., Tireli, A. A., Cesar, P., Corrêa, A. D., Guimarães, I. (2019). Use of an Environmental Pollutant From Hexavalent Chromium Removal as a Green Catalyst in The Fenton Process. *Scientific reports*, 9(1), 12819.

Chang, H., Pannunzio, N. R., Adachi, N., Lieber, M. R. (2017). Non-homologous DNA end joining and alternative pathways to double-strand break repair. *Nature reviews. Molecular cell biology*, 18(8), 495–506.

Claussin, C., Porubský, D., Spierings, D. C., Halsema, N., Rentas, S., Guryev, V., Lansdorp, P. M., Chang, M. (2017). Genome-wide mapping of sister chromatid exchange events in single yeast cells using Strand-seq. *eLife*, 6, e30560.

Cleaver, J. E., Afzal, V., Feeney, L., McDowell, M., Sadinski, W., Volpe, J. P., Busch, D. B., Coleman, D. M., Ziffer, D. W., Yu, Y., Nagasawa, H., Little, J. B. (1999). Increased ultraviolet sensitivity and chromosomal instability related to P53 function in the xeroderma pigmentosum variant. *Cancer research*, 59(5), 1102–1108.

Costa, A. N., Moreno, V., Prieto, M. J., Urbano, A. M., Alpoim, M. C. (2010). Induction of morphological changes in BEAS-2B human bronchial epithelial cells following chronic sub-cytotoxic and mildly cytotoxic hexavalent chromium exposures. *Molecular carcinogenesis*, 49(6), 582–591.

Driscoll, T., Steenland, K., Nelson, D. I., Prüss-Üstün, A., Campbell-Lendrum, D. H. et al. (2004). Occupational carcinogens : assessing the environmental burden of disease at national and local levels / Tim Driscoll ... [et al.]. World Health Organization.

D'Amours, D., Stephen P. J. (2002). The MRE11 Complex: At the Crossroads of DNA Repair and Checkpoint Signalling. *Nature Reviews Molecular Cell Biology* 3(5) 317–27.

Environmental Protection Agency (EPA), (2005). Guidelines for carcinogen risk assessment, EPA/630/P-03/001B Risk Assessment Forum, U.S. Environmental Protection Agency Washington, DC

Gildemeister, O. S., Sage, J. M., Knight, K. L. (2009). Cellular redistribution of Rad51 in response to DNA damage: novel role for Rad51C. *The Journal of biological chemistry*, 284(46), 31945–31952.

Grimsrud, T. K., Berge, S. R., Martinsen, J. I., Andersen, A. (2003). Lung cancer incidence among Norwegian nickel-refinery workers 1953-2000. *Journal of environmental monitoring : JEM*, 5(2), 190–197.

Helleday, T., Nilsson, R., Jenssen, D. (2000). Arsenic[III] and heavy metal ions induce intrachromosomal homologous recombination in the hprt gene of V79 Chinese hamster cells. *Environmental and molecular mutagenesis*, 35(2), 114–122.

Hirose T, Kondo K, Takahashi Y, Ishikura H, Fujino H, Tsuyuguchi M, Hashimoto M, Yokose T, Mukai K, Kodama T, Monden Y. (2002). Frequent

microsatellite instability in lung cancer from chromate-exposed workers. *Molecular Carcinogenesis* 33(3) 172–80

Huang, J., Wu, G., Zeng, R., Wang, J., Cai, R., Ho, J. C., Zhang, J., Zheng, Y. (2017). Chromium contributes to human bronchial epithelial cell carcinogenesis by activating Gli2 and inhibiting autophagy. *Toxicology research*, 6(3), 324–332.

International Agency for Research on Cancer (IARC); (1993). (IARC Monographs on the Evaluation of Carcinogenic Risks to Humans, No. 58.) Available from: <https://www.ncbi.nlm.nih.gov/books/NBK499756/>

Ishikawa, Y., Nakagawa, K., Satoh, Y., Kitagawa, T., Sugano, H., Hirano, T., Tsuchiya, E. (1994). Characteristics of chromate workers' cancers, chromium lung deposition and precancerous bronchial lesions: an autopsy study. *British journal of cancer*, 70(1), 160–166.

Ishikawa, Y., Nakagawa, K., Satoh, Y., Kitagawa, T., Sugano, H., Hirano, T., & Tsuchiya, E. (1994). "Hot spots" of chromium accumulation at bifurcations of chromate workers' bronchi. *Cancer research*, 54(9), 2342–2346.

Jensen R. B., Carreira A., Kowalczykowski S. C. (2010). Purified human BRCA2 stimulates RAD51-mediated recombination. *Nature* 467, 678–683.

Jeyasekharan, A. D., Liu, Y., Hattori, H., Pisupati, V., Jonsdottir, A. B., Rajendra, E., Lee, M., Sundaramoorthy, E., Schlachter, S., Kaminski, C. F., Ofir-Rosenfeld, Y., Sato, K., Savill, J., Ayoub, N., Venkitaraman, A. R. (2013). A cancer-associated BRCA2 mutation reveals masked nuclear export signals controlling localization. *Nature structural & molecular biology*, 20(10), 1191–1198.

Johnson, J., Schewel, L. Graedel, T. E. (2006). The contemporary anthropogenic chromium cycle. *Environmental Science and Technology*, 40(22), 7060-7069.

Kaiser R. F. (1948). The pharmacist's place in cancer control. *Public health reports (Washington, D.C. : 1896)*, 63(35), 1111–1114.

Krawic, C., Zhitkovich, A. (2018). Toxicological Antagonism among Welding Fume Metals: Inactivation of Soluble Cr(VI) by Iron. *Chemical research in toxicology*, 31(11), 1172–1184.

Kieber, R., Eilley, J., Zvalaren, S. (2002). Chromium speciation in rainwater: temporal variability and atmospheric deposition. *Environmental Science and Technology*, 36, 5321-5327.

Langård, S., Vigander, T. (1983). Occurrence of lung cancer in workers producing chromium pigments. *British journal of industrial medicine*, 40(1), 71–74.

Lee, S., Cavallo, L., Griffith, J. (1997). Human p53 binds Holliday junctions strongly and facilitates their cleavage. *The Journal of biological chemistry*, 272(11), 7532–7539.

Levy, L. S., Martin, P. A., Bidstrup, P. L. (1986). Investigation of the potential carcinogenicity of a range of chromium containing materials on rat lung. *British journal of industrial medicine*, 43(4), 243–256.

Li, X., Heyer, W. D. (2008). Homologous recombination in DNA repair and DNA damage tolerance. *Cell research*, 18(1), 99–113.

Marshall, G., Ferreccio, C., Yuan, Y., Bates, M. N., Steinmaus, C., Selvin, S., Liaw, J., Smith, A. H. (2007). Fifty-year study of lung and bladder cancer mortality in Chile related to arsenic in drinking water. *Journal of the National Cancer Institute*, 99(12), 920–928.

Martino, J., Holmes, A. L., Xie, H., Wise, S. S., & Wise, J. P., Sr (2015). Chronic Exposure to Particulate Chromate Induces Premature Centrosome Separation and Centriole Disengagement in Human Lung Cells. *Toxicological sciences: an official journal of the Society of Toxicology*, 147(2), 490–499.

Meaza, I., Speer, R. M., Toyoda, J. H., Lu, H., Wise, S. S., Croom-Perez, T. J., Aboueissa, A. E., Wise, J. P., Sr (2020). Prolonged exposure to particulate Cr(VI) is cytotoxic and genotoxic to fin whale cells. *Journal of trace elements in medicine and biology : organ of the Society for Minerals and Trace Elements (GMS)*, 62, 126562.

Mezynska, M., Brzóška, M. M. (2018). Environmental exposure to cadmium-a risk for health of the general population in industrialized countries and preventive strategies. *Environmental science and pollution research international*, 25(4), 3211–3232.

Occupational Safety and Health Administration (OSHA). *Occupational exposure to hexavalent chromium*. Department of Labor, 2006; Vol. 71, pp 10100–10385.

Prabhu, V. P., Simons, A. M., Iwasaki, H., Gai, D., Simmons, D. T., Chen, J. (2002). p53 blocks RuvAB promoted branch migration and modulates resolution of Holliday junctions by RuvC. *Journal of molecular biology*, 316(5), 1023–1032.

Proctor, D. M., Suh, M., Campleman, S. L., Thompson, C. M. (2014). Assessment of the mode of action for hexavalent chromium-induced lung cancer following inhalation exposures. *Toxicology*, 325, 160–179.

Qin, Q., Xie, H., Wise, S. S., Browning, C. L., Thompson, K. N., Holmes, A. L., & Wise, J. P., Sr (2014). Homologous recombination repair signaling in chemical carcinogenesis: prolonged particulate hexavalent chromium exposure suppresses the Rad51 response in human lung cells. *Toxicological sciences : an official journal of the Society of Toxicology*, 142(1), 117–125.

Quievryn, G., Peterson, E., Messer, J., Zhitkovich, A. (2003). Genotoxicity and mutagenicity of chromium(VI)/ascorbate-generated DNA adducts in human and bacterial cells. *Biochemistry*, 42(4), 1062–1070.

Reynolds, M., Armknecht, S., Johnston, T., Zhitkovich, A. (2012). Undetectable role of oxidative DNA damage in cell cycle, cytotoxic and clastogenic effects of Cr(VI) in human lung cells with restored ascorbate levels. *Mutagenesis*, 27(4), 437–443.

Rodrigues, C. F., Urbano, A. M., Matoso, E., Carreira, I., Almeida, A., Santos, P., Botelho, F., Carvalho, L., Alves, M., Monteiro, C., Costa, A. N., Moreno, V., Alpoim, M. C. (2009). Human bronchial epithelial cells malignantly transformed by

hexavalent chromium exhibit an aneuploid phenotype but no microsatellite instability. *Mutation research*, 670(1-2), 42–52.

Sarto, F., Cominato, I., Bianchi, V., Levis, A. G. (1982). Increased incidence of chromosomal aberrations and sister chromatid exchanges in workers exposed to chromic acid (CrO<sub>3</sub>) in electroplating factories. *Carcinogenesis*, 3(9), 1011–1016.

Sengupta, S., Linke, S. P., Pedoux, R., Yang, Q., Farnsworth, J., Garfield, S. H., Valerie, K., Shay, J. W., Ellis, N. A., Wasyluk, B., Harris, C. C. (2003). BLM helicase-dependent transport of p53 to sites of stalled DNA replication forks modulates homologous recombination. *The EMBO journal*, 22(5), 1210–1222.

Siegel, R. L., Miller, K. D., Jemal, A. (2020). Cancer statistics, 2020. *CA: a cancer journal for clinicians*, 70(1), 7–30.

Siri, S. O., Martino, J., Gottifredi, V. (2021). Structural Chromosome Instability: Types, Origins, Consequences, and Therapeutic Opportunities. *Cancers*, 13(12), 3056.

Sonoda, E., Sasaki, M. S., Morrison, C., Yamaguchi-Iwai, Y., Takata, M., Takeda, S. (1999). Sister chromatid exchanges are mediated by homologous recombination in vertebrate cells. *Molecular and cellular biology*, 19(7), 5166–5169.

Speer, R. M., Wise, S. S., Croom-Perez, T. J., Aboueissa, A. M., Martin-Bras, M., Barandiaran, M., Bermúdez, E., Wise, J. P., Sr (2019). A comparison of particulate hexavalent chromium cytotoxicity and genotoxicity in human and leatherback sea turtle lung cells from a one environmental health perspective. *Toxicology and applied pharmacology*, 376, 70–81.

Speer, R. M., Toyoda, J. H., Croom-Perez, T. J., Liu, K. J., Wise, J. P. (2021). Particulate Hexavalent Chromium Inhibits E2F1 Leading to Reduced RAD51 Nuclear Foci Formation in Human Lung Cells. *Toxicological sciences : an official journal of the Society of Toxicology*, 181(1), 35–46.

Stackpole, M. M., Wise, S. S., Goodale, B. C., Duzevik, E. G., Munroe, R. C., Thompson, W. D., Thacker, J., Thompson, L. H., Hinz, J. M., Wise, J. P., Sr (2007). Homologous recombination repair protects against particulate chromate-induced chromosome instability in Chinese hamster cells. *Mutation research*, 625(1-2), 145–154.

Standeven, A. M., Wetterhahn, K. E. (1992). Ascorbate is the principal reductant of chromium(VI) in rat lung ultrafiltrates and cytosols, and mediates chromium-DNA binding in vitro. *Carcinogenesis*, 13(8), 1319–1324.

Stark, J. M., Pierce, A. J., Oh, J., Pastink, A., Jasin, M. (2004). Genetic steps of mammalian homologous repair with distinct mutagenic consequences. *Molecular and cellular biology*, 24(21), 9305–9316.

Stearns, D. M., Kennedy, L. J., Courtney, K. D., Giangrande, P. H., Phieffer, L. S., Wetterhahn, K. E. (1995). Reduction of chromium(VI) by ascorbate leads to chromium-DNA binding and DNA strand breaks in vitro. *Biochemistry*, 34(3), 910–919.

Takahashi, Y., Kondo, K., Ishikawa, S., Uchihara, H., Fujino, H., Sawada, N., Miyoshi, T., Sakiyama, S., Izumi, K., Monden, Y. (2005). Microscopic analysis of the

chromium content in the chromium-induced malignant and premalignant bronchial lesions of the rat. *Environmental research*, 99(2), 267–272.

Tessier, D. M., Pascal, L. E. (2006). Activation of MAP kinases by hexavalent chromium, manganese and nickel in human lung epithelial cells. *Toxicology letters*, 167(2), 114–121.

Toya, T., Fukuda, K., Kohyama, N., Kyono, H., Arito, H. (1999). Hexavalent chromium responsible for lung lesions induced by intratracheal instillation of chromium fumes in rats. *Industrial health*, 37(1), 36–46.

Wiktor-Brown, D. M., Sukup-Jackson, M. R., Fakhraldien, S. A., Hendricks, C. A., Engelward, B. P. (2011). p53 null fluorescent yellow direct repeat (FYDR) mice have normal levels of homologous recombination. *DNA repair*, 10(12), 1294–1299.

Wilson, D. M., 3rd, Thompson, L. H. (2007). Molecular mechanisms of sister-chromatid exchange. *Mutation research*, 616(1-2), 11–23.

Wise J.P. Sr, Orenstein J.M., Patierno S.R. (1993) Inhibition of lead chromate clastogenesis by ascorbate: Relationship to particle dissolution and uptake. *Carcinogenesis* 14: 429–434, 1993

Wise J.P. Sr, Wise S.S. and Little J.E. (2002).The cytotoxicity and genotoxicity of particulate and soluble hexavalent chromium in human lung cells. *Mutation Research* 517(1-2):221-9.

Wise, S. S., Schuler, J. H., Holmes, A. L., Katsifis, S. P., Ketterer, M. E., Hartsock, W. J., Zheng, T., & Wise, J. P., Sr (2004a). Comparison of two particulate hexavalent chromium compounds: Barium chromate is more genotoxic than lead chromate in human lung cells. *Environmental and molecular mutagenesis*, 44(2), 156–162.

Wise, S. S., Elmore, L. W., Holt, S. E., Little, J. E., Antonucci, P. G., Bryant, B. H., Wise, J. P., Sr (2004). Telomerase-mediated lifespan extension of human bronchial cells does not affect hexavalent chromium-induced cytotoxicity or genotoxicity. *Molecular and cellular biochemistry*, 255(1-2), 103–111.

Wise, S. S., Holmes, A. L., Wise, J. P., Sr (2006). Particulate and soluble hexavalent chromium are cytotoxic and genotoxic to human lung epithelial cells. *Mutation research*, 610(1-2), 2–7.

Wise, J. P., Sr, Wise, S. S., Holmes, A. L., LaCerte, C., Shaffiey, F., Aboueissa, A. M. (2010a). The cytotoxicity and genotoxicity of hexavalent chromium in Stellar sea lion lung fibroblasts compared to human lung fibroblasts. *Comparative biochemistry and physiology. Toxicology & pharmacology : CBP*, 152(1), 91–98.

Wise, S. S., Holmes, A. L., Qin, Q., Xie, H., Katsifis, S. P., Thompson, W. D., Wise, J. P., Sr (2010b). Comparative genotoxicity and cytotoxicity of four hexavalent chromium compounds in human bronchial cells. *Chemical research in toxicology*, 23(2), 365–372.

Wise, S. S., Aboueissa, A. E., Martino, J., Wise, J. P., Sr (2018). Hexavalent Chromium-Induced Chromosome Instability Drives Permanent and Heritable Numerical and Structural Changes and a DNA Repair-Deficient Phenotype. *Cancer research*, 78(15), 4203–4214.

Wong, V., Armknecht, S., Zhitkovich, A. (2012). Metabolism of Cr(VI) by ascorbate but not glutathione is a low oxidant-generating process. *Journal of Trace Elements in Medicine and Biology*, 26(2), 192-196.

Wu, F., Sun, H., Kluz, T., Clancy, H. A., Kiok, K., Costa, M. (2012). Epigallocatechin-3-gallate (EGCG) protects against chromate-induced toxicity in vitro. *Toxicology and applied pharmacology*, 258(2), 166–175.

Xiaohua L., Yanshuang S., Li W., Yuhui L., Ji Z., Yanhui M., Yun W., Wenjun M., Lei Y., Guang J. (2012). Evaluation of the correlation between genetic damage and occupational chromate exposure through BNMN frequencies. *Journal of occupational and environmental medicine* 54(2):166–170.

Xie, H., Holmes, A. L., Wise, S. S., Gordon, N., Wise, J. P., Sr (2004). Lead chromate-induced chromosome damage requires extracellular dissolution to liberate chromium ions but does not require particle internalization or intracellular dissolution. *Chemical research in toxicology*, 17(10), 1362–1367.

Xie, H., Wise, S. S., Holmes, A. L., Xu, B., Wakeman, T. P., Pelsue, S. C., Singh, N. P., Wise, J. P., Sr (2005). Carcinogenic lead chromate induces DNA double-strand breaks in human lung cells. *Mutation research*, 586(2), 160–172.

Xie, H., Holmes, A. L., Wise, S. S., Huang, S., Peng, C., Wise, J. P., Sr (2007). Neoplastic transformation of human bronchial cells by lead chromate particles. *American journal of respiratory cell and molecular biology*, 37(5), 544–552.

Xie, H., Wise, S. S., Wise, J. P., Sr (2008). Deficient repair of particulate hexavalent chromium-induced DNA double strand breaks leads to neoplastic transformation. *Mutation research*, 649(1-2), 230–238.

Xie, H., Holmes, A. L., Young, J. L., Qin, Q., Joyce, K., Pelsue, S. C., Peng, C., Wise, S. S., Jeevarajan, A. S., Wallace, W. T., Hammond, D., Wise, J. P., Sr (2009). Zinc chromate induces chromosome instability and DNA double strand breaks in human lung cells. *Toxicology and applied pharmacology*, 234(3), 293–299

Xie, H., Holmes, A. L., Wise, S. S., Young, J. L., Wise, J. T., Wise, J. P., Sr (2015). Human Skin Cells Are More Sensitive than Human Lung Cells to the Cytotoxic and Cell Cycle Arresting Impacts of Particulate and Soluble Hexavalent Chromium. *Biological trace element research*, 166(1), 49–56.

Yao, Y., & Dai, W. (2014). Genomic Instability and Cancer. *Journal of carcinogenesis & mutagenesis*, 5, 1000165.

Zhang, F., Paramasivam, M., Cai, Q., Dai, X., Wang, P., Lin, K., Song, J., Seidman, M. M., & Wang, Y. (2014). Arsenite binds to the RING finger domains of RNF20-RNF40 histone E3 ubiquitin ligase and inhibits DNA double-strand break repair. *Journal of the American Chemical Society*, 136(37), 12884–12887.

Zhitkovich, A., Quievryn, G., Messer, J., & Motylevich, Z. (2002). Reductive activation with cysteine represents a chromium(III)-dependent pathway in the induction of genotoxicity by carcinogenic chromium(VI). *Environmental health perspectives*, 110 Suppl 5(Suppl 5), 729–731.

## CURRICULUM VITAE

Idoia Meaza Isusi

Wise Laboratory of Environmental and Genetic Toxicology  
University of Louisville  
500 S Preston Street  
Tower 55A, Room 1403  
Louisville, KY 40292  
502-3091245  
Idoia.isusi@louisville.edu

### **Education:**

- 2019-2024 M.S./Ph.D. in Pharmacology and Toxicology at the University of Louisville (KY).
- 2016-2018 M.S. in Marine Environment and Resources at the University of the Basque Country, Southampton University and University of Liege.
- 2012-2016 B.S. in Biology at the University of the Basque Country (EHU/UPV).

### **Professional Experience:**

- 2013-2016 Undergraduate internship in the Research Centre for Experimental Marine Biology at the University of the Basque Country (EHU/UPV).
- 2019-2020 Visiting Scholar/Research Assistant at Wise Laboratory of Environmental and Genetic Toxicology.
- 2019-2024 Research Assistant at Wise Laboratory of Environmental and Genetic Toxicology under the M.S./Ph.D. program.

### **Honors, Awards and Professional Activities:**

- 2018-2016 Erasmus Mundus Scholarship for the M.S. Marine Environment and Resources.
- 2019 Third place, poster presentation award, (Idoia Meaza), Ohio Valley Chapter of the Society of Toxicology
- 2020 Awarded Graduate Student Council Research Grant in Fall 2020.
- 2021 Awarded Environmental Carcinogenesis Merit Award for Graduate Students by the Carcinogenesis Specialty Section, Society of Toxicology.
- 2021 Awarded to 1<sup>st</sup> place 3 Minute Thesis presentation in the Ph.D category at the Virtual Summer Meeting OVSOT 2021.

### **Professional Memberships & Societies:**

Society of Toxicology (SOT) since 2019

Society for the Study and Conservation of Marine Fauna (AMBAR) since 2013

Spanish Society of Cetaceans (SEC), since 2017.

### **Continuing Education Coursework**

2021	Carcinogenesis Specialty Section (Society of Toxicology), webinar series "Fundamentals and Frontiers in Carcinogenesis"
2021	CE04: Concepts and Approaches for Current and Future Metals Toxicological Research, Society of Toxicology Annual Meeting 2021
2018-2020	Pharmacology and Toxicology Department seminar series.
2017	Scientific Diving Course.
2017	Advanced seminars in Environmental Ethics and Ethical Perspectives of Climate Change: Multicultural Perspectives on Ethics and Environment.
2016	Theoretical and Practical Course on Cytogenetics and Cell Cultures.
2015	Aquaculture seminar series.
2014-2016	Annual course for the volunteer network of AMBAR, for the attendance to strandings and monitoring of marine mammals, sharks and turtles.
2013	Course in ecology of marine birds, turtles and mammals.

### **Field Work**

2018	Conducted alligator sampling expedition at Kennedy Space Center (NASA).
2018	Conducted whale sample collecting in the Gulf of Maine, in fall season. Biopsies were taken from fin, humpback and minke whale.
2017	Scientific diving census on fauna and flora and processing, taxa identification and data analysis in Stareso Marine Station in Consica.
2017	Scientific diving census on fauna and flora in the Basque coast.
2015-2017	Conducted mussel sampling in the Basque coast and mussel dissection at the lab.
2014-2018	Conducted whale and small cetacean necropsy and sample collection under the collaboration between NGO AMBAR and the Research Centre for Experimental Marine Biology at the University of the Basque Country (EHU/UPV).
2014-2018	Conducted marine mammal census in the basque coast under the NGO AMBAR.

### **Publications**

1. Wise, J. P., Jr, Croom-Perez, T. J., **Meaza, I.**, Aboueissa, A. M., López Montalvo, C. A., Martin-Bras, M., ... Wise, J. P., Sr (2019). A whale of a tale: A One Environmental Health approach to study metal pollution in the Sea of

Cortez. *Toxicology and applied pharmacology*, 376, 58–69.  
doi:10.1016/j.taap.2019.05.005

2. **Meaza I.**, Speer M.R., Toyoda, J.H., Lu H., Wise S.S. Croom-Perez J.T., El-Makarim, A. and Wise, Sr., J. P. Prolonged exposure to particulate Cr(VI) is cytotoxic and genotoxic to fin whale cells [published online ahead of print, 2020 May 26]. *J Trace Elem Med Biol.* 2020;62:126562.  
doi:10.1016/j.jtemb.2020.126562
3. **Meaza, I.**, Toyoda, J. H., & Wise Sr, J. P. (2021). Microplastics in Sea Turtles, Marine Mammals and Humans: A One Environmental Health Perspective. *Frontiers in Environmental Science*, 8(298). doi:10.3389/fenvs.2020.575614
4. Speer, M.R., **Meaza I.**, Toyoda, J.H, Lu, Y., Xu, Q., Walter, R., Kong, M., Wise, Sr., J.P. Particulate hexavalent chromium alters microRNAs in human lung cells that target key carcinogenic pathways. Submitted to Environmental Science and Technology

### **Abstracts:**

1. **Meaza I.**, Ruiz, L., Gardeazabal, P. Izagirre U., Lekube, X., Soto M., New marine mammal catalogue in the Biscay Bay Environmental Bioespecimen Bank. Scientific Poster on the International Conference of on Environmental Specimen Bank, Bilbao 2-4 October 2017.
2. Atxaga, O., Arbelo, M., Izagirre, U., Ruiz, L., Fernandez, A., Lekube, X., Soto, M., **Meaza, I.**, and Sierra, E., Anatomopathological study of cases of the network of stranding of marine mammals of the Basque Country. Scientific Poster on the Congress of Spanish Society of Cetaceans (SEC), Bilbao, 18-21 October 2018.
3. Atxaga, O., Arbelo, M., Izagirre, U., Ruiz, L., Fernandez, A., Lekube, X., Soto, M., **Meaza, I.**, and Sierra, E. Remote retrospective histopathological analysis of stranded marine mammals' samples by means of the use of in silico stored histological HR digital images: a pilot experience in Biscay Bay. European Society of Biomaterials ESB2019, Germany.
4. **Meaza I.** and Wise J.P. Sr., The Impact of Acute and Prolonged Exposure of Particulate Hexavalent Chromium in Fin Whale and Humpback Whale Cells. Presented at MSc Thesis in Marine Environment and Resources Erasmus Mundus Master, 6-7 September 2018, Plentzia-Spain.
5. **Meaza I.** and Wise J.P. Sr., Characterization of the Toxicological Effects of Particulate Hexavalent Chromium in Fin Whale and Humpback Whale Primary Cell Cultures. Presented at Congress of Spanish Society of Cetaceans (SEC), Bilbao, 18-21 October 2018.
6. Croom-Pérez, T.J., **Meaza Isusi, I.**, Ziemba, C.R., Anglin, C.T., Wise Sr., J. P. (2019) The Cytotoxic and Genotoxic Effect of Prolonged Particulate Hexavalent Chromium Exposure on Human Lung Epithelial Cells. 58th Annual Meeting of the Society of Toxicology (Baltimore, Maryland).
7. Wise, Jr., J.P., Croom-Perez, T.J., **Meaza, I.**, Montalvo, C.L., Wise, C.F., Wise, S.S., Wise, J.T.F., Speer, R.M., Abouiezza, A., Bras, M.M., Savery, L.C., Urbán, J., Young, J.L., and Wise, Sr., J.P. A Whale of a Tale: A One

Environmental Health Approach to Study Metal Pollution in the Sea of Cortez. *Toxicological Sciences*, 168(1): 3431, 2019.

8. **Meaza I.**, Speer, M.R., Toyoda, J.H. and Wise J.P. Sr. Particulate Hexavalent Chromium Induces Cytotoxicity and Genotoxicity in Female and Male Fin Whale Primary Cells. Presented at Research Louisville, 10-12 September 2019, Louisville-KY.
9. Croom-Perez, T.J., **Meaza, I.**, and Wise, Sr., J.P. Chromate-Induced Changes in the Fibroblast Secretome and its Effects on Epithelial Cells. Presented at Research!Louisville, Louisville, Kentucky, 2019
10. Wise, S.S., Miller, E., Daniel, S., **Meaza, I.**, Toyoda, J.H., Lu, H., Speer, R. M., Young, J. L., Isakov, R., Jagggers, H., Wise, Jr., J. P., Croom-Perez, T. J., Cai, L., Hoyle, G., and Wise, Sr., J. P. Effects of Chronic Exposure to Particulate Chromate in Rat Lungs. Presented at Research!Louisville, Louisville, Kentucky, 2019
11. **Meaza I.**, Speer, M.R., Toyoda, J.H. and Wise J.P. Sr. Particulate Hexavalent Chromium Induces Cytotoxicity and Genotoxicity in Female and Male Fin Whale Primary Cells. Presented at Ohio Valley Regional Chapter of the Society of Toxicology (OVSOT), Cincinnati. Ohio, October 2019. ( 3<sup>rd</sup> place Poster Award)
12. Croom-Perez, T.J., **Meaza, I.**, and Wise, Sr., J.P. Chromate-Induced Changes in the Fibroblast Secretome and its Effects on Epithelial Cells. Presented at the annual meeting of the Ohio Valley Regional Chapter of the Society of Toxicology (OVSOT), Cincinnati. Ohio, October 2019.
13. Wise, Jr., J.P., Lu, H., **Meaza, I.**, Wise, S.S., Croom-Perez, T., Speer, R., Toyoda, J., Ali, A., Cai, L., Liu, K.J., Wise, J.T.F., Young, J.L., and Wise, Sr., J.P. An Environmental Toxicology Assessment of Heavy Metal Accumulation in American Alligators in Florida. Presented at the Ohio Valley Chapter of the Society of Toxicology (OVSOT) annual meeting, October 2019.
14. **Meaza I.**, Speer, M.R., Toyoda, J.H. and Wise J.P. Sr. The Characterization of Toxicological Effects of Particulate Hexavalent Chromium in Female and Male Fin Whale Cells. Presented at the first World Marine Mammal Conference, 8-12 December 2019, Barcelona, Spain .
15. Wise, Sr., J.P., Wise, Jr., J.P., Toyoda, J.H., Croom-Perez, T.J., Aboueissa, A., , Montalvo, C.L., **Isusi, I.M.**, Wise, S.S., Wise, C.F., Wise, J.T.F., Li Chen, T., Perkins, C.R., Bras, M.M., Speer, R.M., and Urbán, J. Of Whales and Men: Understanding Metal Pollution in the Sea of Cortez through a One Environmental Health Approach. Presented at the World Marine Mammal Science Conference, Barcelona, Spain, December, 2019.
16. **Meaza, I.**, Speer, M. R, Toyoda, H. J. and Wise, Sr., J.P. Particulate Hexavalent Chromium Induces Cytotoxicity and Genotoxicity in Female and Male Fin Whale Primary Fibroblasts. Presented at the Ohio Valley Chapter of the Society of Toxicology (OVSOT) annual meeting, October, 2019.
17. **Meaza, I.**, Speer, R.M, Toyoda, J.H. and Wise, Sr., J.P. Particulate Hexavalent Chromium Induces Cytotoxicity and Genotoxicity in Female and Male Fin Whale Cells. *Toxicological Sciences*, 174(1): 2565, 2020.

18. Croom-Perez, T., Young, J.L., Xu, J., **Meaza, I.**, Lu, H. Wise, S.S., Cai, L., and Wise, Sr., J.P. Characterizing a Mouse Model for the Effects of Whole Life, Low Dose Cadmium Exposure, and High Fat Diet on the Lung. *Toxicological Sciences*, 168(1): 3430, 2020.
19. Wise, Jr., J.P., Lu, H., Toyoda, J.H., Speer, R.M., Croom-Perez, T., **Meaza Isusi, I.**, Wise, S.S., Young, J.L. Tan, Y., Hoyle, G., Isakov, R., Jaggars, H., Wise, Sr., J.P., and Cai, L. Genotoxicity in the Heart-Brain Axis Following Inhalation of Hexavalent Chromium [Cr(VI)] in a Rat Model. *Toxicological Sciences*, 174(1): 3130, 2020.
20. **Meaza I.**, Speer M.R., Toyoda, J.H., Lu H., Wise S.S. Croom-Perez J.T., El-Makarim, A. and Wise, Sr., J. P. Prolonged exposure to particulate Cr(VI) is cytotoxic and genotoxic to fin whale cells at Ohio Valley Chapter of the Society of Toxicology (OVSOT) Student & Postdoctoral Researchers' Virtual Summer Meeting, Tuesday July 28<sup>th</sup>, 2020
21. Williams, A.R., Speer, R.M., Browning, C. **Meaza, I.**, Toyoda J., and Wise, Sr., J. P. Particulate Hexavalent Chromium Inhibits DNA Repair by Targeting RAD51 Paralogs at Ohio Valley Chapter of the Society of Toxicology (OVSOT) Student & Postdoctoral Researchers' Virtual Summer Meeting, Tuesday July 28<sup>th</sup>, 2020
22. **Meaza, I.**, Speer, R.M., Toyoda, J.H., Lu, Y., Xu, Q., Walter, R., Kong, M. and Wise, Sr., J.P. Particulate Hexavalent Chromium Altered the Expression of miRNAs Involved in Carcinogenesis Pathways. Ohio Valley Chapter of the Society of Toxicology (OVSOT) annual meeting, November, 2020.
23. Williams, A.R., Speer, R.M., Browning, C. **Meaza, I.**, Toyoda J., and Wise, Sr., J. P. Particulate Hexavalent Chromium Inhibits DNA Repair by Targeting RAD51 Paralogs. Presented at the Ohio Valley Chapter of the Society of Toxicology (OVSOT) annual meeting, November, 2020.
24. **Meaza, I.**, Speer, R.M., Toyoda, J.H., Lu, Y., Xu, Q., Walter, R., Kong, M. and Wise, Sr., J.P. Particulate Hexavalent Chromium Altered the Expression of miRNAs Involved in Carcinogenesis Pathways. *Toxicological Sciences*, 180(S1):2073, 2021.
25. Williams, A.R., Speer, R.M., Browning, C. **Meaza, I.**, Toyoda J., and Wise, Sr., J. P. Particulate Hexavalent Chromium Inhibits DNA Repair by Targeting RAD51 Paralogs. Society of Toxicology, March 2021.
26. **Meaza, I.**, Speer, R.M., Toyoda, J.H., Lu, Y., Xu, Q., Walter, R., Kong, M. and Wise, Sr., J.P. Particulate Hexavalent Chromium Induces Global miRNA Downregulation and Altered the Expression of miRNAs Involved in Carcinogenesis Pathways. Genetic Toxicology Association, May 5<sup>th</sup> 2021.
27. Williams, A.R., Speer, R.M., Browning, C. **Meaza, I.**, Toyoda J., and Wise, Sr., J. P. Particulate Hexavalent Chromium Inhibits DNA Repair by Targeting RAD51 Paralogs. Genetic Toxicology Association, May 4<sup>th</sup> 2021.
28. **Meaza, I.**, Speer, R.M., Toyoda, J.H., Lu, Y., Xu, Q., Walter, R., Kong, M. and Wise, Sr., J.P. Particulate Hexavalent Chromium [Cr(VI)] Exposure Alters miRNA Profiles and Targets miRNAs Involved in Pathways of Cr(VI)

Carcinogenesis, at Ohio Valley Chapter of the Society of Toxicology (OVSOT) Student & Postdoctoral Researchers' Virtual Summer Meeting, Wednesday July 28<sup>th</sup>, 2021

29. **Meaza, I.**, Toyoda, J.H., Lu, H., Williams, A.R., Wise, S.S., and Wise Sr. J.P. Particulate Hexavalent Chromium Induces Loss of RAD51 Leading to Increased Genomic Instability, A Driver of Carcinogenesis. EMGS September 22-25 2021.
30. **Meaza, I.**, Toyoda, J.H., Lu, H., Williams, A.R., Wise, S.S., and Wise Sr. J.P. Particulate Hexavalent Chromium Targets RAD51, the Key Protein in Homologous Recombination Repair, Leading to Increased Genomic Instability, A Driver of Carcinogenesis. Research Louisville! October 25-29 2021.
31. Hoang, L., Meaza I. and Wise Sr. J.P. Particulate Cr(VI) Targets Separase in Human Lung Cells. Research Louisville! October 25-29 2021.

#### **Presentations:**

- 2016 Final degree project defense "Comparative histology of different tissue samples obtained from different marine mammal species beached in the Basque Coast during 2015-2016." Dr. Urtzi Izagirre and Idoia Meaza, University of the Basque Country
- 2018 Master Thesis defense: Idoia Meaza Isusi and Dr. John P. Wise "The Impact of Acute and Prolonged Particulate Hexavalent Chromium Exposure in Fin Whale and Humpback Whale Cells".
- 2020 Seminar in Pharmacology and Toxicology Department in April .
- 2021 3 Minute Thesis at the Annual Society of Toxicology: Meaza I. Save the Whales; A Solution to a Climate in Crisis! Presented at the 3 Minute Thesis competition organized by Society of Toxicology (SOT), in the Annual Conference 2021 (Virtual).
- 2021 Seminar in Pharmacology and Toxicology Department in June.
- 2021 Guest Lecture for the course Marine Conservation, University of Southern Mississippi, invited by Dr. Virginia Schweiss
- 2021 3 Minute Talk Poster Presentation at Genetic Toxicology Association, May 5<sup>th</sup> 2021. **Meaza, I.**, Speer, R.M., Toyoda, J.H., Lu, Y., Xu, Q., Walter, R., Kong, M. and Wise, Sr., J.P. Particulate Hexavalent Chromium Induces Global miRNA Downregulation and Altered the Expression of miRNAs Involved in Carcinogenesis Pathways.
- 2021 3 Minute Thesis, Ohio Valley Chapter of the Society of Toxicology (OVSOT) Student & Postdoctoral Researchers' Virtual Summer Meeting, Wednesday July 28<sup>th</sup>, 2021 **Meaza, I.**, Speer, R.M., Toyoda, J.H., Lu, Y., Xu, Q., Walter, R., Kong, M. and Wise, Sr., J.P. Particulate Hexavalent Chromium [Cr(VI)] Exposure Alters miRNA Profiles and Targets miRNAs Involved in Pathways of Cr(VI) Carcinogenesis

**Teaching experience:**

- 2015 Seminar for the Annual Course of Strandings for AMBAR volunteers “Histological procedures used with the samples collected from the strandings in the Basque Coast during the 2015 and possible first steps for a sampling protocol”
- 2016 Lecture for the Biocultural integrity course of the Marine Environment and Resources Master “Strandings of Marine Mammals and plastics”.
- 2017 Lecture for the Biocultural integrity course of the Marine Environment and Resources Master “Strandings of Marine Mammals and plastics”.
- 2018 Seminar for the Congress of Spanish Society of Cetaceans, 18- 21 October Bilbao 2018 “The Histological Processing of Samples of Stranded Cetaceans in The Basque Coast; a Collaboration Between AMBAR and PiE-UPV/EHU”
- 2021 Guest Lecture for the course Marine Conservation, University of Southern Mississippi, invited by Dr. Virginia Schweiss

**Mentoring/Training Experience:**

- 2018 Trained three undergraduate students .
- 2019 Trained one undergraduate student
- 2021 Served as a Judge in the Louisville Regional Science and Engineering Fair 2021 and trained one undergraduate student (Lily Hoang)

**Leadership Experience:**

- 2019-2020 Graduate student representative (class matriculated in 2019) in Pharmacology and Toxicology
- 2020-2021 Graduate student representative (class matriculated in 2019) in Pharmacology and Toxicology
- 2021-2022 Graduate student representative (class matriculated in 2019) in Pharmacology and Toxicology
- 2021-2022 Director of Graduate Travel Grants in the Graduate Student Council at University of Louisville